Masteroppgave

NTNU
Norges teknisk-naturvitenskapelige universitet
Fakultet for informasjonsteknologi og elektroteknikk
Institutt for teknisk kybernetikk

Jon Eirik Lisle Andresen

Haptic Feedback for Hydraulic Hand Prosthesis

Masteroppgave i Kybernetikk og Robotikk
Veileder: Geir Mathisen
Juni 2019

NTNU
Kunnskap for en bedre verden

Jon Eirik Lisle Andresen

Haptic Feedback for Hydraulic Hand Prosthesis

Masteroppgave i Kybernetikk og Robotikk
Veileder: Geir Mathisen
Juni 2019

Norges teknisk-naturvitenskapelige universitet
Fakultet for informasjonsteknologi og elektroteknikk
Institutt for teknisk kybernetikk

NTNU
Kunnskap for en bedre verden

Til Bjørg Helene og Ervin.
Jammen klarte vi ikke dette også.

NTNU
Norwegian University
Of Sience and Technology

Faculty if Information Technology and Electrical Engineering,

Department of Engineering Cybernetics

Master's Thesis

Student name: Jon Eirik Lisle Andresen

Field: Engineering Cybernetics

Tittel (norsk): Haptisk tilbakekobling for hydraulisk håndprotese

Title (English): Haptic feedback for hydraulic hand prosthesis

Description:
The Norwegian firm Hy5 AS develops upper limb prostheses for people with a congenital condition or who have suffered a traumatic amputation of their hand and parts of their arm. To provide the user with a best possible starting point for controlling the prostheses accurately, adding sensory capabilities to the prosthetic hand as well as implementing some form of haptic feedback is desired. This means that information about for example forces, velocities and/or joint angles within the prosthesis is conveyed using one or more forms of stimulation (mechanical or electrical). In theory, this can restore parts of the mechano sensory abilities lost as a result of the amputation or congenital condition.

Stepwise, this is the task:

1. Perform a literature review to acquire knowledge of previously attempted sensory and haptic feedback systems, as well as methods for evaluating such system's function. This shall include sensor types, number and placement, how information gathered from the sensors are interpreted in a micro controller, and how and which information is conveyed to the user of the prosthesis.
2. Propose and describe a system that can be built onto the Hy5 hand. This shall include what parts the system shall consist of and what is required to combine them into a working system.
3. Make a working system as described in step 2, mounted on a prosthetic hand, if possible, a Hy5 hand. To the degree possible, the system is to be constructed with the whole prosthetic system, including the control system, in mind.
4. Evaluate the system using the method(s) found in step 1.

Supervisor(s): Geir Mathisen, Department of Engineering Cybernetics, NTNU
Bjøn Olav Bakka, Hy5 AS
Anders Fougner, Department of Engineering Cybernetics, NTNU
Øyvind Stavdahl, Department of Engineering Cybernetics, NTNU

Trondheim, 11. January 2019

Geir Mathisen
Main Supervisor

NTNU
Norges teknisk-naturvitenskapelige universitet

Fakultet for informasjonsteknologi og elektroteknikk
Institutt for teknisk kybernetikk

Masteroppgave

Studentens navn:	Jon Eirik Lisle Andresen
Fag:	Teknisk kybernetikk
Tittel (norsk):	Haptisk tilbakekobling for hydraulisk håndprotese
Tittel (English):	Haptic feedback for hydraulic hand prosthesis

Beskrivelse:
Det norske selskapet Hy5 AS utvikler håndproteser for mennesker med medfødt misdannelse eller traumatisk amputasjon av hånden og eventuelt deler av armen. For å gi brukeren et best mulig utgangspunkt for å styre bevegelsene i protesen nøyaktig, ønsker en å implementere sensorikk i hånden og en form for haptisk tilbakekobling. Det betyr at informasjon om f.eks. krefter, hastigheter og/eller leddvinkler i protesen formidles til brukeren gjennom en eller flere former for stimulering (mekanisk eller elektrisk). I prinsipp kan dette gjenoppretter deler av den mekanosensoriske evnen som er tapt på grunn av amputasjonen.

Konkret blir oppgaven:

1. Gjøre en litteraturstudie for å innhente informasjon om tidligere utprøvde sensor- og haptisk tilbakekoblings-systemer, samt metoder for å evaluere funksjonen til slike systemer. Dette skal omfatte sensortyper, antall og plasseringer, hvordan informasjonen fra sensorene er tolket i en mikrokontroller, og hvordan og hvilken informasjon som formidles til brukeren av protesen.
2. Foreslå og beskrive et system som kan bygges på Hy5 hånda. Dette skal omfatte hvilke enheter systemet skal bestå av og hva som skal gjøres for å sette disse sammen til et fungerende system.
3. Lag et fungerende system slik beskrevet i punkt 2, montert på en håndprotese, om mulig på en Hy5 hånd. I den grad det er mulig skal systemet konstrueres med hele systemet, inkludert styringssystemet, i tankene.
4. Evaluer systemet i henhold til metoden(e) funnet i punkt 1.

Veileder(e): Geir Mathisen, Institutt for teknisk kybernetikk, NTNU
Bjøn Olav Bakka, Hy5 AS
Anders Fougner, Institutt for teknisk kybernetikk, NTNU
Øyvind Stavdahl, Institutt for teknisk kybernetikk, NTNU

Trondheim, 11. Januar 2019

Geir Mathisen
Faglærer

Abstract

In cooperation with the Norwegian company Hy5, haptic feedback for their prosthetic hand is explored in this thesis. The first parts of the paper are a literature review and a theory section presenting haptic feedback, human motor control and tactile sensation. Based on those findings, and a previous specialisation project, see Appendix D, a haptic feedback system is proposed, assembled, partially mounted on a Hy5 hand, programmed and tested.

While the resulting system provides insights and a stepping stone for future research, several of the system requirements were not meet. The main source of system failure was the poor performance of the force sensors when integrated with with the prosthetic hand. Future work includes ensuring better force sensing, particularly at low contact forces, and more functional testing in more realistic settings.

Sammendrag

I samarbeid med det norske selskapet Hy5 utforskes haptisk tilbakekobling for deres håndprotese i denne oppgaven. Rapportens første deler er et litteraturstudie og en teoridel hvor haptisk tilbakekobling, menneskelig bevegelsesstyring og berøringssans presenteres. Det er basert på disse funnene, og et fordypningsprosjekt, se Appendix D, at et system for haptisk tilbakekobling beskrives, konstrueres, delvis monteres på en Hy5 håndprotese, programmeres og testes.

Selv om det resulterende systemet gir innsikt og danner en vei videre for videre studier oppnås ikke flere av kravene satt til system. Hovedkilden til problemene var kraftsensorenes svake ytelse etter integrering med håndprotesen. Videre arbeid omfatter bedre kraftdeteksjon, spesielt ved små kontaktkrefter, og mer funksjonell tesing i mer realistiske settinger.

Preface

This thesis concludes my studies at the engineering cybernetics programme at NTNU. This project is a continuation of my specialisation project completed in 2018 and parts of that work was used in this project, see references to Andresen (2018). That project and this master thesis were in cooperation with the Norwegian company Hy5.

Throughout this semester, I have received useful help and guidance from my main supervisor Geir Mathisen at the Department of Engineering Cybernetics, for which I am very grateful. For help with the prosthesis lab at NTNU and for other prosthesis related challenges and questions, I would like to thank co-supervisors Anders Fougner and Øyvind Stavdahl, both also at the Department of Engineering Cybernetics. I would also like to thank Hy5 and everyone there who have been eager to help, answer questions and provide resources. In particular, I would like to thank co-supervisor Bjørn Olav Bakka at Hy5 for his help and guidance.

Omega Verksted at NTNU has also proven to be of great help during this semester and I would like to extend my thanks to everyone there eager to help and answer even the most basic questions. I would also like to thank my co-MSc student for putting up with my messy lab habits and for discussions and help throughout the semester.

A big thank-you is also owed to friends and family members who at a moments notice dropped everything to help when this thesis was about to get the better of me. Related to this report, help with planning and proof reading has been extremely helpful. That the following pages contain anything is just as much your achievement as it is mine.

To run the Hy5 hand at the lab, I used software provided for a past course, TTK26 with minor modifications. As a part of Atmel Studio, the IDE used for software development, the Advanced Software Framework (ASF) from Microchip, provided some of the modules used when creating the software for the system. However, while the functions and modules found in Appendix A use code provided through ASF, the code was written by me.

The rest of the report and associated code, figures and hardware is the result of my own work.

Approved: _____

Main Supervisor: Geir Mathisen.
Trondheim 24.06.2019

TABLE OF CONTENTS

Problem Description i

Problemstilling ii

Summary iii

Sammendrag iii

Preface iv

Table of Contents ix

List of Figures xii

List of Tables xiv

Abbreviations xv

1 Introduction 1

1.1 Powered Upper Limb Prostheses 1

1.2 Hy5 Hand 1

1.3 Haptic Feedback in Upper Limb Prostheses 2

1.4 Prosthesis Lab at NTNU 3

1.5 Motivation 3

1.6 Limitations 4

2 Literature Review 5

2.1 Non-Invasive, Temporally Discrete Feedback of Object Contact and Release Improves Grasp Control of Closed-Loop Myoelectric Transradial Prostheses. Clemente et al. (2016) . . . 5
2.2 Adding Vibrotactile Feedback to a Myoelectric-Controlled Hand Improves Performance when Online Visual Feedback is Disturbed. Raveh et al. (2018) . . . 6
2.3 Vibrotactile Display, Perception, Technology and Applications. Choi and Kuchenbecker (2013) . . . 6
2.4 Summaries of Select Previous Systems . . . 7
2.4.1 Investigation of a cognitive strain on hand grasping induced by sensory feedback for myoelectric hand, Yamada et al. (2016). . . . 7
2.4.2 Relaying the High Frequency Contents of Tactile Feedback to Robotic Prosthesis Users: Design, Filtering, Implementation and Validation, Fani et al. (2019). . . . 8
2.4.3 A Cosmetic Prosthetic Digit with Bioinspired Embedded Touch Feedback, Barone et al. (2017). . . . 8
2.4.4 The Impact of Simultaneously Applying Normal Stress and Vibrotactile Stimulation for Feedback of Exteroceptive Information, Motamedi et al. (2017) . . . 9
2.5 Components . . . 9
2.5.1 Sensors . . . 9
2.5.2 Controlling Units . . . 10
2.5.3 Algorithms . . . 11
2.5.4 Actuators . . . 11
2.6 Evaluation Methods . . . 12
2.6.1 Virtual Eggs Test . . . 12
2.6.2 Component Testing . . . 12
2.6.3 Day to Day Use . . . 12

3 Theory **13**
3.1 Sensation in Human Skin . . . 13
3.1.1 Force and Contact Detection in Glabrous Skin . . . 13
3.1.2 Vibration Detection in Hairy Skin . . . 14
3.2 Human Motor Control . . . 14
3.3 Force Sensitive Resistors . . . 15

4 Specification **17**
4.1 Sensor Requirements . . . 17
4.1.1 Force Sensor . . . 17
4.1.2 Inertial Measurement Unit / Accelerometer . . . 19
4.1.3 Angle Measurement . . . 20
4.2 MCU Requirements . . . 21
4.2.1 Speed and Time Usage . . . 21
4.2.2 Communication . . . 21
4.2.3 IO . . . 21
4.2.4 Size and Weight . . . 22
4.3 Actuator Requirements . . . 22
4.3.1 For Discrete Event Sensory Control Feedback . . . 22
4.3.2 For Force-level Feedback . . . 22
4.3.3 For Texture Recognition . . . 22
4.4 Acceptance Requirements for the Complete System . . . 23

5 Proposed Architecture **25**
5.1 Force Feedback . . . 25
5.1.1 Force Sensor . . . 25
5.1.2 Controlling Unit . . . 26
5.1.3 Actuators . . . 26
5.1.4 Algorithm . . . 26
5.2 Deformation Detection . . . 26
5.2.1 Angle Sensors . . . 26
5.2.2 Algorithm . . . 27
5.3 Software Architecture . . . 27

6 Implementation **29**
6.1 List of Components . . . 29
6.2 Implementation of Hardware . . . 30
6.2.1 Powering the Hy5 Hand . . . 30
6.2.2 Construction . . . 30
6.2.3 Structure of Electronics . . . 31
6.2.4 Armband for Vibrotactile Actuators . . . 35
6.2.5 Sensor Mounting on Hy5 Hand . . . 36
6.2.6 Encoders . . . 38
6.3 Software . . . 39

7 Test Methodology **45**
7.1 LRA Compatibility with EMG . . . 45
7.2 Force Sensitivity Testing . . . 46
7.3 Vibration Sensation Testing . . . 47
7.3.1 Minimum Perceivable Amplitude . . . 47
7.3.2 Minimum Perceivable Difference in Amplitude . . . 47
7.3.3 Discrete Pulse Testing . . . 47
7.4 Power Consumption . . . 48
7.5 Grip Testing . . . 48
7.6 Deformation Testing . . . 49

8 Results **51**
8.1 Vibration Sensation Testing . . . 51
8.1.1 Single Site Pulse Testing . . . 51
8.1.2 Dual Site Pulse Testing . . . 53
8.1.3 Vibration Amplitude Testing . . . 56
8.2 FSR response . . . 58
8.3 Cost . . . 61
8.4 Power Consumption . . . 62
8.5 LRA compatibility with EMG . . . 63
8.6 Grip Testing . . . 65
8.7 Deformation Detection . . . 66

9 Discussion **67**
9.1 LRA Compatibility with EMG . . . 67
9.2 Vibration Sensation Testing . . . 67
9.2.1 Single Site Pulse Testing . . . 68
9.2.2 Dual Site Pulse Testing . . . 68
9.2.3 Minimum Perceivable Amplitude . . . 69
9.2.4 Minimum Perceivable Difference in Amplitude . . . 69
9.3 FSR response . . . 70
9.4 Power Consumption . . . 70
9.5 Grip Testing . . . 71
9.6 Deformation Testing . . . 71
9.7 Hardware . . . 72
9.7.1 Force Sensors . . . 72
9.7.2 Angle Sensors . . . 72

9.7.3 Motor Drivers 73
9.7.4 Actuators and Armbands 73
9.7.5 MCU and Evaluation Board 73
9.8 Software 74
9.9 Cost 74
9.10 Acceptance Requirements 74

10 Conclusion and Future Work **77**
10.1 Conclusion 77
10.2 Future Work 77

Bibliography **78**

Appendix A Code **83**

Appendix B Pictures of Hardware **89**

Appendix C Overview of Attached Files **97**

Appendix D Specialisation Project **99**

LIST OF FIGURES

6.1 Schematic overview of the electronic hardware of the feedback system. . 31

6.2 Schematic overview of the motor drivers (Texas Instruments DRV2605) and LRA (Jinlong Machinery & Electronics G0832012). R0, R1, R2, D0, D1 and D2 form the solution to the I2C address clash mentioned in 6.2.2. 32

6.3 Schematic overview of the FSR force sensors (Interlink Electronics FSR400). 33

6.4 Schematic overview of the FSR force sensors (Interlink Electronics FSR400) after extra sensors were added to the index and middle fingers to increase the active area of the sensors. 34

6.5 Schematic overview of one of the two encoder sets placed on the finger joints of the Hy5 hand (ams AS5134-ZSST). Note that Q1 and R16 represent a shared transistor resistor pair for both the encoder sets and thus power is controlled for all the encoders simultaneously. 35

6.6 Class diagram showing the structure of the developed code. Class names correspond to names of header and C files, see appendix A. Red classes are modules provided through ASF 40

6.7 Sequence of system start-up with user opting not to calibrate sensors, but rely on data stored from a previous calibration. If there is no stored data, default values are used. 41

6.8 Sequence of FSR calibration routine. 42

6.9 State diagram showing the haptic_feedback_state_machine responsible for the main application. Pulse control block is shown in figure 6.10. 43

6.10 State diagram showing the Pulse Control block from figure 6.9. 44

8.1 Graph showing FSR resistance as a function of weight applied to a small point, as described in section 7.2. 59
8.2 Graph showing FSR resistance as function of weight applied evenly over the active area of the sensor, as described in section 7.2. 59
8.3 Graph showing FSR resistance as function of weight applied evenly over the active area of the sensor when covered by a piece of a dish-washing glove, as described in section 7.2. 60
8.4 Graph showing FSR resistance as function of weight applied evenly over the active area of the sensor when covered by a piece of a artificial skin, as described in section 7.2. 60
8.5 Raw EMG signals with no LRA present. 63
8.6 Raw EMG signals with LRA present, running at maximum amplitude. . . 64
8.7 Raw EMG signals with a strong muscle contraction starting close to the middle of the plot. 64

10.1 Picture of the evaluation board. 89
10.2 Picture of the low pass filters, in the top left, shown schematically in figure 6.5. In the lower left, the voltage dividers for the FSRs, as shown schematically in figure 6.4, are placed. 90
10.3 Picture of the motor drivers, I2C control and reset button. The motor drivers are shown schematically in figure 6.2. The orange, blue and green cables to the very right connect to the actuators in the armband. 91
10.4 Picture of the Hy5 hand with all sensors mounted. The black, white, green and yellow cables coming from the middle and index fingers are connected to the force sensors. The other cables are for the encoders. 92
10.5 Picture of the Hy5 hand with all sensors mounted. The thumbs proximal encoder would be placed on the opposite side of the distal, had it not fallen off before this photo was taken. 92
10.6 Picture of the first armband. 93
10.7 Picture of the second armband. 93
10.8 Picture of the first armband, worn on the upper arm. 94
10.9 Picture of the second armband, worn on the upper arm. 94
10.10 Picture of the second armband, worn on the upper arm. 95

LIST OF TABLES

8.1 Table showing the results of the single vibration test for the first arm band. During these trials, a 100% success rate was observed. 52
8.2 Table showing the results of the single vibration test for the second arm band. During these trials, a 100% success rate was observed. 53
8.3 Table showing the results of the dual vibration test performed on the first armband. Mismatches are indicated by dark grey fields 54
8.4 Table showing the results of the dual vibration test performed on the second armband. Mismatches are indicated by dark grey fields. 55
8.5 Results of the minimum detectable amplitude, as described in section 7.3.1, using the first armband. 56
8.6 Results of the minimum detectable amplitude, as described in section 7.3.1, using the second armband. 56
8.7 Results of the test performed to determine the minimum discernible amplitude, as described in section 7.3.2 using the first armband. The same test was run twice. 56
8.8 Results of the test performed to determine the minimum discernible amplitude, as described in section 7.3.2 using the second armband. The test was run two times, but with different base amplitudes. 57
8.9 Table showing the results of the sensitivity test described in section 7.2. . 58
8.10 Table showing the cost of components, excluding passives such as resistors, capacitors, diodes and wires. All prices except for 3D printing and the elastic band is collected from Digikey.no. All prices are in NOK. . . . 61
8.11 Test of subsystem power consumption under different conditions. 62
8.12 Results of grip test as described in section 7.5. 65

8.13 Results of deformation test as described in section 7.6. 66

Abbreviations

EMG	=	Electromyography
CNS	=	Central Nervous System
PNS	=	Peripheral Nervous System
FA	=	Fast Adapting
SA	=	Slow Adapting
MCU	=	Micro Controller Unit
FSR	=	Force Sensing Resistor
DESC	=	Discrete Event Sensory Control
IO	=	Input and Output
ERM	=	Eccentric Rotating Mass
PWM	=	Pulse Width Modulation
IMU	=	Inertial Measurement Units
ADC	=	Analogue-to-Digital Converter
IMU	=	Inertial Measurement Unit
ADC	=	Analogue to Digital Converter
IC	=	Integrated Circuit
LRA	=	Linear Resonant Actuator
PCB	=	Printed Circuit Board
VI	=	Virtual Instrument
PSU	=	Power Supply Unit
ISR	=	Interrupt Service Routine

CHAPTER

ONE

INTRODUCTION

1.1 Powered Upper Limb Prostheses

The following section is adopted from Andresen (2018).

State of the art powered upper limb prostheses, used due to amputation or a congenital condition, have their basis in electromyography (EMG). Using electrodes, placed on the skin of the residual limb of a prosthesis user, electrical impulses that travel along a muscle as it contracts can be recorded and used as a control signal for the prosthetic hand or arm. Such prostheses give the user a clear control path, but lacks a direct feedback loop, other than visual inspection or incidental cues from changes motor noise and vibration.

1.2 Hy5 Hand

The following section is adopted from Andresen (2018).

The Hy5 hand is made by the Norwegian company Hy5 based in Oslo and Raufoss. With their product, Hy5 aims to provide more functionality, but at a lower cost, than prosthetic hands with multiple electric motors. Movement of the Hy5 hand's fingers is powered by hydraulics, giving the hand a strong and robust grip. Using a series of springs and wires,

the digit that is experiencing the least amount of resistance will move the most. This also ensures that the more proximal digit will move into contact with an object, before the distal digit closes in. This adaptive grip allows the hand to close around objects of varying shapes and sizes.

The hand is powered by a single electric motor running two pumps. One pump is a high volume, low pressure pump, while the other is a low volume, high pressure pump. Having different pumps ensures that not only speedy finger movement when freely moving. but also a high griping force, are possible.

Using EMG sensors as input, the rate of closing the fingers is controlled by controlling the speed of the motor. The direction of movement is controlled by electrically operated valves. The opening of the hand is mainly caused by springs in the fingers pulling them back once the hydraulic pressure drops.

1.3 Haptic Feedback in Upper Limb Prostheses

For a thorough review of haptic feedback in upper limb prostheses, see Antfolk et al. (2013b).

Haptic feedback provides a user of a device or a service with real or perceived, mechanical stimuli to convey information. This can be achieved using vibration, shear forces, normal forces, electrical stimuli or something else. An example many will be familiar with outside the realm of prostheses is the vibrating motors commonly found in mobile phones.

In the case of upper limb prosthesis, the information one might wish to convey to the user can include contact forces, slip, joint angles, deformation, texture properties, temperature or others. To this end, a prosthetic hand can be fitted with sensors and a way of processing their outputs. To then close the control loop, the nervous system of the user of the prosthesis must be interfaced with. This can be done by interacting with the skin mechanically or electrically, interacting directly with the nerve endings in the peripheral nervous system (PNS), or in the extreme, one can imagine interacting directly with some part of the central nervous system (CNS).

The following section is adopted from Andresen (2018). The information provided to the user is said to be modality matched when the measured quantity matches the modality in which the stimulation is given. Otherwise, the feedback is said to use sensory substitution. In addition to modality, the perceived location of the stimuli can be considered. When

the correct perceived location is stimulated the feedback achieves somatotopic matching. This matching can be achieved by either stimulating the nervous system directly, or by stimulating phantom maps sometimes present on the residual limb Antfolk et al. (2013a).

1.4 Prosthesis Lab at NTNU

The Department of Engineering Cybernetics at NTNU has a lab dedicated to upper limb prostheses. At the time of writing, it can be found in room D0043 in the basement of the department building. The lab includes equipment for running and evaluating a prosthetic hand compatible with the Otto-Bock quick connection, as well as other projects and equipment.

The setup for running a prosthetic hand in the lab is as follows. Wireless EMG sensors from Delsys can be used to record muscle activity. From their base station, the recorded signals are transmitted over USB to a laptop computer. Running on that computer is a National Instruments LabView Virtual Instrument (VI). There are several available choices for which control scheme to use. There exists a system based on on-screen sliders and buttons, for quick testing and debugging. Another system is based proportional control using two or four sensors, depending on the required degrees of freedom. A third option is based around pattern recognition and user training to control the hands opening, closing, pronation and supination.

The processed control signals are transmitted from the computer to the connected hand through a National Instruments cDAQ 9191. A rechargeable battery pack is available For powering hands at the lab. However, as discussed in 6.2.1, the Hy5 hand draws too much current for that battery, leading to a drop in voltage, further leading to the hand entering a limbo state. Therefore, to power the Hy5 hand, an external power supply able to deliver up to $6\mathrm{A}$ or current at $7.5\mathrm{V}$, is needed. For the duration of this project, such a PSU was borrowed from the department workshop.

1.5 Motivation

The following two paragraphs are adopted from Andresen (2018)

Much of what a normal human hand provides is lost when lacking its sensory function. This is also true for hand prostheses. While many currently commercially available pros-

thetic hands provide a high level of finger dexterity and advanced control, there are none that provide the user with dedicated feedback.

Providing users with haptic feedback can increase embodiment Marasco et al. (2011), reduce phantom pain Dietrich et al. (2012) and increase the usability of a prosthesis without relying on visual monitoring Schoepp et al. (2018). Haptic feedback is also a frequently requested feature by users Cordella et al. (2016). Having haptic feedback could provide Hy5 with a commercial advantage over their competitors.

In Andresen (2018), aspects of haptic feedback was researched and explored. This thesis is a continuation of that work, where a system will be designed, built and tested to further explore haptic feedback for the Hy5 hand.

1.6 Limitations

The system created and discussed in this thesis will not consider the following:

- **Industrialization.** The feedback and sensory systems presented are clearly prototypes, and are not trivial to manufacture. How to make the proposed system commercially viable or ready for mass production is not considered in this report.
- **Control.** While parts of the system proposed might be useful in a more refined control scheme, the control of the prosthesis will not be considered.
- **Internal pressures.** Measuring the pressure in the hydraulic fluid in the hand could be an alternative to measuring contact forces. This will not be considered in this report.
- **Power Supply.** When using the a prosthetic hand, one needs to carry a power source. To use the feedback and sensory system, integration with this power supply or adding a second power source would be required. Other than recording the power requirements of the system, powering the system is not considered in this report.

CHAPTER

TWO

LITERATURE REVIEW

This chapter presents some key systems and articles before presenting a summary of components, algorithms and evaluation methods.

2.1 Non-Invasive, Temporally Discrete Feedback of Object Contact and Release Improves Grasp Control of Closed-Loop Myoelectric Transradial Prostheses. Clemente et al. (2016)

In an attempt to restore to the ability to utilise discrete events as the main source of information in motor control, Clemente *et.al* created a system where information about contact and release between the fingers of a myoelectric prosthesis and an object is conveyed to the user through short, vibrotactile pulses. The system consists of two thimbles, one placed over the thumb, and one placed over the index and middle fingers. Within the thimbles, FSRs were embedded, and cables led the signal from the sensors to a wearable arm cuff, which houses a micro controller unit as well as the vibrating motors used for actuation.

The system was tested by five prosthesis users. They tested the system over a series of training and evaluation sessions. The users were also given the system to use in their

daily activities. Validation of the systems performance was done by moving fragile boxes, emulating eggs, over a barrier. Both a reduction in force and the time to complete the task was observed during the trials.

The main complaints from the users were in regards to the cosmetics and bulkiness of the device. Despite these shortcomings three of the five users decided to keep and use the system after the trials were completed.

2.2 Adding Vibrotactile Feedback to a Myoelectric-Controlled Hand Improves Performance when Online Visual Feedback is Disturbed. Raveh et al. (2018)

To evaluate the effect of adding force feedback through vibrotactile stimulation to a hand prosthesis, Raveha *et.al* performed functional tests under three different conditions: one with full visual feedback, one with vibrotactile feedback in darkness, and one without vibrotactile feedback in darkness.

The system consisted of force sensors placed in the inner part of a gripper style hand prosthesis. Force readings were processed by a controlling circuit which activated vibrotactile actuators placed in a band placed around the users arm.

The sum of the force levels from the sensors were used as the input signal. After calibration, five force levels were defined and for each level, a set number of actuators would activate.

The results of the trials showed that the vibrotactile feedback and visual feedback yielded similar mean times to complete the task, both significantly shorter than with no feedback. Errors were also reduced when vibrotactile feedback was enabled, but the error rate was still lowest with full visual feedback.

2.3 Vibrotactile Display, Perception, Technology and Applications. Choi and Kuchenbecker (2013)

Vibrotactile displays are one or more actuators which can stimulate the skin of the user. Stimulation can be done by either a single channel or multiple channels. When consid-

ering both single channel and multi channel sites, the minimum perceptible stimuli is of high importance. A description of the perceived power of a stimulation intensity I is given by Stevens power law $\psi(I) = kI^e$. Where ψ is the perceived intensity, I is the physical intensity, k is a positive constant ,and e determines the growth rate of the perceived magnitude, ranging from 0.35 to 0.86. e depends on stimulation conditions, especially frequency. Sensitivity, as a function of frequency, follows a u-shape between 150 Hz and 300 Hz.

Human tactile sensation has sufficient temporal resolution to distinguish between pulses with a separation as short as 5 ms.

In their review, Choi and Kuchenbecker compared different classes of vibrotactile actuators. The following table is an adoption of that work.

Actuator type	**Affordability and Avaliability**	**Mechanical Simplicity**	**Electrical Simplicity**	**Customisability**	**Expressiveness**
Generic Voice Coil	Medium	Medium	Medium	Medium	Medium
Vibrotactile Voice Coil	Low	Low	Medium	High	High
ERM Motor	High	High	High	Low	Low
Piezoelectric Actuator	Low	Medium	Low	Medium	High

2.4 Summaries of Select Previous Systems

2.4.1 Investigation of a cognitive strain on hand grasping induced by sensory feedback for myoelectric hand, Yamada et al. (2016).

To determine the cognitive load induced by adding sensory feedback to a prosthetic hand, an FSR was fastened to the thumb of a prosthetic hand. Three vibrators, VTM-003 from Yatsugatake Club, were placed on the upper arm of the subjects. No controlling unit is mentioned. Actuators were controlled by a PWM-signal, and force levels or finger angles were communicated by either stimulating different sites or on a single site with different stimulation intensity levels.

For several of their test subjects, Yamada concludes that feedback can reduce congnitive

strain induced by using a prosthetic device. This is especially true for users adept at controlling the prosthesis. Yamada also concludes that one stimulator which changes in intensity creates less cognitive strain than spatially changed, i.e information is conveyed by which actuator is running, simulators.

2.4.2 Relaying the High Frequency Contents of Tactile Feedback to Robotic Prosthesis Users: Design, Filtering, Implementation and Validation, Fani et al. (2019).

This system attempts to give users of prosthetic hands the ability to determine roughness of surfaces. Two inertial measurement units (IMU), MPU-9250 Motion Tracking Devices. In addition to other properties, these record acceleration in three dimensions. The control board is based on Cypress Programmable System on Chip. The controlling unit includes a separate, higher voltage circuit to power the actuators. Linear voice coils were chosen in this setup.

The signal from the IMUs was filtered and processed such that only contact information as well as texture information would activate the actuators. After filtering, the sum of the amplitude of signal values were combined to act as the input to the actuators.

To be able control both frequency and amplitude independently of one another, the NCC01-04-001-1X Voice Coil Actuator (H2W Technologies) was chosen to create vibration. This actuator can create a range of frequencies and amplitudes, while maintaining low power usage and space requirements, but at a relatively high monetary cost.

2.4.3 A Cosmetic Prosthetic Digit with Bioinspired Embedded Touch Feedback, Barone et al. (2017).

To give a cosmetic digit more functionality, contract information is transmitted to the user via vibrotactile feedback. The sensor placed in the tip of the prosthesis is an FSR. As the only task of the system was to vibrate at contact and at release, the controlling component was a custom, analogue circuit, rather than a micro-controller. This allows for simple and quick information transmission. To provide vibration, an ERM coin motor (model 31-113, Precision Microdrives Ltd), was chosen. The whole system was embedded in polymer, and included the ability to wirelessly charge the battery through induction.

2.4.4 The Impact of Simultaneously Applying Normal Stress and Vibrotactile Stimulation for Feedback of Exteroceptive Information, Motamedi et al. (2017)

In a study of applying both vibrotactile and normal force stimulation on skin under different conditions, Motamedi et. al experimented with applying both types of stimulation simultaneously. The two stimulation methods were applied at the same location during some trial and at different locations, 6 cm apart, during others.

In their study, Motamedi et. al concluded that adding vibrotactile stimulation degrades the quality of applied normal stimulation. This degradation was present even when the vibration was applied at a different site than the normal stimulation. However, the opposite was found for the quality of vibrotactile stimulation when normal and vibrotactile stimulation was applied at the same site. Both quantitative and subjective reports from test candidates reported this. The cause of the increase was assessed to be that an increase in normal force pressed the vibrators deeper into the skin and thus less of the vibrational energy was dissipated before reaching the appropriate nerve endings.

A Precision Microdrives MN: 310–113 was used for the vibrotactile feedback . For normal force stimulation, a custom piston solution was created.

2.5 Components

The following section is a short summary of some types of components used as sensors, controller and actuators.

2.5.1 Sensors

For a review of other sensors suitable for use in haptic feedback for upper limb prostheses see Chapell (2011).

Force Sensors

Force Sensitive Resistors are piezoresistive sensor. The resistance of the flat FSR drops as pressure is applied to its surface. Using a voltage divider and an ADC, the force can be

read by a MCU. FSRs are inaccurate and best suited for a qualitative rather than absolute and quantitative force measurement. When covered and not exposed to large shear forces they are quite durable. FSRs were placed on the fingertips of systems such as described in Barone et al. (2017) and Clemente et al. (2016). For a more in depth look at FSR's, see section 3.3.

Capacitive Sensors sensors can be used when a higher degree of accuracy is needed. While more accurate, linear and with less hysteresis than an FSR, a capacitive sensor is generally more expensive and requires more complex circuitry to use. In Schoepp et al. (2018), a capacitive sensor from the manufacturer SingeTact is used in a force feedback system where force readings are used to control tactors creating a normal force on the skin of the user.

Texture Sensors

Accelerometer or Inertial Measurement Units fastened in or on the fingertips of a prosthetic hand can be used in texture sensing. They can record the acceleration induced by the movement of the hand. Using filtering, one can remove the components of the signal not created by surface roughness. In Fani et al. (2019), IMUs are fastened to the fingers of the prosthetic device. The high frequency content of the filtered and summed 3D acceleration was used for texture recognition.

2.5.2 Controlling Units

Desktop computers are used in many setups as a way of demonstrating a concept or an algorithm. However, programs or code written in such a way are only suitable for demonstration and early prototyping and cannot be used in a mobile, real life scenario.

Custom circuitry can be made when little processing of the sensor signal to create output is required. An example was used in Barone et al. (2017) where a hysteresis was the only data processing that happens between the sensor and actuator. Such systems are simple, cheap and add little delay between input and output, but lack expressive power and customisability.

Micro controllers are used in most systems. A MCU offers flexibility and expressive power at some monetary cost and potentially reduced speed compared to simple custom

circuits. Systems such as Fani et al. (2019) and Schoepp et al. (2018) are examples.

2.5.3 Algorithms

Continuous force feedback is provided in Schoepp et al. (2018). A mapping between sensory reading and actuator levels will give users a way to continuously gauge contact force without relying on visual feedback.
Discrete event feedback is a simpler force feedback scheme where only events are conveyed. In Barone et al. (2017) contact and release events trigger a vibrating motor to signal the events.

2.5.4 Actuators

Linear tactors/pressure pads create a constant downwards force onto the skin of the user. In Schoepp et al. (2018) custom actuators were created and embedded within a prosthesis socket. In Antfolk et al. (2012), air pressure created at the fingertips created pressure at pads placed on the residual limb of the user.

Eccentric rotating mass vibration motors spin at a high frequency. By having mass offset from the centre of rotation, vibrations are induced. Such actuators create vibrations at a set frequency. A small coin version is used in Barone et al. (2017). Such actuators are cheap and widely available, however, they lack expressiveness and often require some extra housing.

Linear resonant actuators are similar in function to rotating mass motors. However, instead of creating vibrations by rotating, LRAs create vibrations tangential to their mounting surface. The motion is caused by moving a magnet attached to a spring up and down with an alternating current. The resonant frequency is determined by the relationship between the mass and spring, and thus the frequency of operation is limited to a narrow band around this resonant frequency. As with rotating motors, LRAs are cheap and widely available. As LRAs cannot be driven by a simple DC current, special motor drivers are necessary to control and power these.

Voice coils are similar in operation to LRAs but in addition to amplitude the frequency of oscillation can be freely controlled, providing a wider range of perceived stimuli. An example, where texture roughness and contact information are recorded and given to the user, is found in Fani et al. (2019).

2.6 Evaluation Methods

2.6.1 Virtual Eggs Test

To evaluate the effectiveness of a their feedback system in Clemente et al. (2016), a modification of a box and block test named The Virtual Eggs Test (VET) was created and utilised. Instead of simply moving a block from one place to another without looking, the VET uses fragile, hollow paper boxes with mechanical fuses, made from spaghetti, with a breaking force of $\sim 11\text{N}$. Over a period of five weekly sessions, the participants in the study were asked to move the fragile boxes over a 15cm high wall, with and without the feedback system active.

2.6.2 Component Testing

To evaluate the components used in a feedback system, their performance in a ideal setting as well as in the setup intended, should be evaluated both before and during design and construction. For example, in Clemente et al. (2016), force sensors were tested both before and after being embedded within a thimble like structure.

The determine which force sensor was most applicable to the proposed setup in Schoepp et al. (2018), several sensors were evaluated. This included confirming what was reported in the data-sheets as well as the sensor behaviours during different loading characteristics.

2.6.3 Day to Day Use

As an addition to the quantitative tests in Clemente et al. (2016), the five subjects of the tests were allowed to use the system during their daily activities. While it might be more difficult to extract hard quantitative data from a questionnaire or interview, letting users test the performance of a product in a as realistic setting as possible can be viewed as the ultimate test of a systems feasibility and performance.

CHAPTER

THREE

THEORY

3.1 Sensation in Human Skin

Human skin can be divided into two main types; glabrous and hairy. The hairy is by far the most abundant by area and is found on most of the human arm. The fingertips, however, are covered in glabrous skin. The two types contain different types of nerve endings, and consequently their sensory abilities are not equivalent.

3.1.1 Force and Contact Detection in Glabrous Skin

As discussed in Andresen (2018), human glabrous skin contains four main receptor types. These can be divided along their receptive fields or along their adaption rates. Receptors with rapid adaption rates, Meissner corpuscles and Pacinian corpuscles, are sensitive to dynamic pressures and forces, i.e vibrations.

Static forces are detected by the slower adapting Merkel cells and Ruffini endings. These detect static forces, shapes and, to a degree, texture.

3.1.2 Vibration Detection in Hairy Skin

Vibration detection and discrimination in human hairy skin, for example the proximal region of the arm, is not as sensitive as the glabrous skin found in the fingertips Merzenich and Harrington (1969). The difference between the minimum amplitude detectable in hairy and glabrous skin at lower frequencies is significant, at around a factor of 5. This difference has a falling trend with increasing frequency, at least up till 200 Hz Mahns et al. (2005). The ability to discern between different stimulation frequencies Δf becomes poorer with an increase in frequency, but the Weber Fraction ,i.e. $\frac{\Delta f}{f}$, remains similar, with a downwards trend for an increase in frequency, for frequencies $f \in [20, 50, 100, 200]$ Hz Mahns et al. (2005).

Similar to in glabrous skin, high frequency tactile sensing is the responsibility of Pacinian corpuscles. In addition to these, hairy skin is also equipped with Hair Follicle Afferent, which detect frequencies lower than 80Hz.

3.2 Human Motor Control

During manipulation of objects, humans rely on a primarily predictive approach, rather then using continuous feedback Johannson and Edin (1993). When moving an object, the brain uses previously created internal models of control to predict the actions required by the body and executes these via the PNS. The role of tactile sensation in such a scheme is twofold.

Events detected by the PNS is encoded and transmitted to the CNS, where performance of the object manipulation can be monitored Johansson and Flanagan (2009). These events include object touch, lift, touchdown and release. Events such as these form the sub goals of a manipulation task. When reaching for an object, the first sub goal is to create a stable grasp of the object. Once an object has been touched, the firing rates of the afferent nerves in the fingers transmit both the force magnitude and the direction of the force applied. The next sub-goal is to create a stable grasp of the object. Maintaining a stable grasp is a balancing act between applying enough tangential force to overcome gravity and not applying an excessive normal force. Information about friction properties of an object is gained during the primary gripping phase, as well as form previous encounters with a similar object. Visual cues also represent a way of determining the surface properties of an object. A mismatch between an expected outcome and the sensed outcome will result

in a corrective action being taken Johansson and Flanagan (2009), such as a change in the gripping force or lift speed. During lifting and holding, the stability is maintained by using signals from the PNS Gentilucci et al. (1997).

The second role is to update the internal models used by the CNS Kawato (1999). This includes updating the expected weight and gripping forces required to lift or move an object. Thus, cues such as visual familiarity and texture recognition can be used to predict the necessary steps required in manipulating an object Johannson and Edin (1993).

Human motor control relies on the predictive scheme as control based on continuous feedback would be far to slow to complete most tasks, as the time delay between the onset of an event and corrective action being taken is inherently long.

3.3 Force Sensitive Resistors

A force sensitive resistor (FSR) is a piezoresisitve, two wire sensor Dahiya et al. (2010). The sensor consists of two layers, separated by a spacer which creates an air gap. The active layer has two sets of interdigitated fingers, like two combs pressed together face to face without legs touching, made of a highly conductive material, e.g a silver alloy. The top layer is coated with a carbon based FSR ink Electronics (2019).

When no force is applied to the sensor, the two layers are separated by air and can be regarded as an open circuit, $R \geq 10\mathrm{M}\Omega$. Once an external pressure is applied to either layer, one or more of the legs of the active layer is shorted by the ink coated layer, leading to a significant drop in overall resistance, typically $R \approx 100\mathrm{k}\Omega$. Thereafter, the resistance of the sensor falls according to an inverse power law, $R_{FSR} \approx \frac{1}{F}$. However, eventually the sensor will reach a saturation point, where no further significant decrease in resistance will occur. This saturation point depends on the exact geometry and makeup of the sensor.

FSRs suffer from large hysteresis and a non linear response. There is also a relatively high variability between individual sensors of the same model and type, consequently individual sensor calibration is especially recommended. The sensors respond rapidly, with a rise time of $\leq 3\mu$s, Electronics (2019). Their resistive nature also makes them highly immune to electromagnetic disturbances. The sensor is flat, with a small spacial footprint, requiring little space outside its active area and that required for the two connecting wires.

CHAPTER

FOUR

SPECIFICATION

4.1 Sensor Requirements

4.1.1 Force Sensor

Power Consumption

Ideally, the sensors should have no power draw when not in use. Additionally, the sensors should use as little as possible when active.

Size

To fit within, or on, the finger of a prosthetic hand, a force sensor must be fairly small. The width of the index and middle finger pad is around 1.5 cm and with length around 4cm. The thumb pad is 2 cm wide and 3.5 cm long. Any sensors placed on the finger pads should have an active field as close to the area of the pad as possible as while remaining physically within the same area.

If the sensor is to be placed on the finger, the thickness of the sensor is especially important. The thickness of the sensor should be comparable to a cosmetic glove worn, on the order

of a few mm.

Another approach is to embed the sensor within the plastic finger of the prosthesis. This will increase the volume available for the sensor as well as making integration with the hand simpler.

Resolution and Range

The Hy5 hand has a maximum tripod grip of 60 N Hy5 (2017). Any sensor needs to survive at least such forces, and ideally have an operating range such that the whole range of forces possible from the hand is covered. To mimic the sensitivity of the human finger tips, a sensor would need to detect forces as small, or smaller than $110\mathrm{mN}$ Kaczmarek et al. (1991).

In previous studies using force feedback, users have been able to successfully discriminate between several force levels, such as in Yamada et al. (2016).

If the resulting system should imitate the DESC, as described in section 3.2, the transitions between control events is the most important output of the sensory system. Thus, sensitivity to first contact is essential. If other events than contact and release are to be used by the system, both shear and normal forces have to be recorded.

Response Time

The time for a stimulus of an afferent ending to move to the cuneate nucleus is at least 14 ms Johansson and Flanagan (2009). It is assumed that to enable the user to have a sense of embodiment of the prosthesis, the time added by the feedback system should be kept as low as possible, around 3-5 ms. Antfolk et al. (2013b). Thus the time from a change in force applied to the sensor to a change in force reading should be kept as low or lower than 3-5 ms. Preferably, the sensor should have a response time lower than 3 ms to allow for time consumption by other parts of the feedback system.

Durability and Resistance to Environment

The Hy5 hand is rated to operate within a temperature range of $5°\mathrm{C}$ to $35°\mathrm{C}$, and a feedback system should be able to operate within at least an as large range. For use outdoors

during a Nordic winter, the lower temperature bound should be lowered, especially considering the distal location of the sensors.

Dividing the force levels into n levels, the maximum drift due to temperature, within the specified acceptable temperature range, should be less than 10% of the size of an interval.

4.1.2 Inertial Measurement Unit / Accelerometer

In addition to contact and release events, lift-off and replace events are crucial in the DESC manipulation scheme. As seen in Fani et al. (2019), these can also be used to determine texture.

Power Consumption

As the accelerometers would not be used when there is no contact forces detected, the system needs to be able to shut these of completely when no touch is detected by the system. The sensor should be powered by ≤ 5 V.

Size

The sensors, inlucding their housing and cabling, will have to fit within the digit of the prosthetic hand. This means fitting within a 0.7mm diameter cylinder. For prototyping, ensuring that small enough components are available might have to suffice, and the sensors can be fastened on the nail side of the finger, though this will interfere with some configurations of the hands adaptive grip.

Resolution and Range

To detect the high frequency tactile information generated when sliding a finger across a surface, the sensor needs to pick up signals with frequencies at least as high as 400 Hz Fani et al. (2019). This requires a sampling rate of at least 800 Hz.

Durability and Resistance to Environment

While requiring the same temperature and humidity resistance as the force sensor, the IMU will ideally be embedded in a part of the finger less prone to mechanical shock, requiring less robustness. However, to accurately measure the vibration from shear and contact forces, the IMU needs a solid and rigid connection to the finger body.

4.1.3 Angle Measurement

Size

To fit on the Hy5 hand's digits, the angle sensors would ideally be embedded within the digits themselves. For prototyping, however, it is sufficient to place the sensors externally on the joints of the digits. Due to the proximity of the middle and index fingers, placing sensors on the middle finger might prove difficult without the embedding mentioned, therefore only two sensors will be considered in this project.

Power Consumption

When not in use, i.e when there is no contact, power usage should be close to 0W. Otherwise, the power usage should be as low as possible.

Resolution and Range

The finger joints of the Hy5 hand is limited to a movement range of $\leq 100^\circ$ and thus the angle sensors need the same range.

For detecting deformation, a reading of absolute angle is not necessary, only change in angle. For this reason, keeping track of the recorded angle is not necessary, nor is it necessary to calibrate the hand to move the digits and angle sensors to a defined position.

4.2 MCU Requirements

4.2.1 Speed and Time Usage

Keeping the signal transmission from sensor to actuator low is in large part the responsibility of the MCU component of the system. The system should record sensor data from all sensors, process the data, and finish transmission to the actuators within, preferably 3-5 ms, and at least within 10 ms.

4.2.2 Communication

For debugging and other purposes, the Hy5 hand includes a Bluetooth module. Through this module, multiple data is available, for example the control signal from the myosensors and RPM of the motor. The hand can also be controlled remotely by sending opening and closing commands. Therefore, to acquire these signals, the MCU unit should include a Bluetooth module, or at least the ability for an external module to be added.

For debugging and development, USB communication is preferred for its universal adoption and ease of use.

4.2.3 IO

The MCU must handle both analogue and digital inputs, with sufficient AD-channels to support multiple sensor inputs.

To drive the vibrotactile actuators, the MCU has to deliver a range of voltages, or be able to drive an external powering circuit.

For the FSR sensors, at least three analogue inputs are needed, and ADC channels to convert the readings into a usable form. For other sensors, either additional analogue ports or a digital bus can be used.

For driving actuators, a simple analogue output is possible. Other options include PWM-controllers or digital interfaces such as I2C. A controller would need at to communicate with at least three actuators, using either dedicated lines or a bus.

4.2.4 Size and Weight

A common request from users of powered prostheses is a reduction of weight Cordella et al. (2016). Therefore the weight of the complete system should be minimised. The size of the controlling MCU should be sufficiently small so as to allow for embedding into the socket of the prosthetic arm, or, if the particular socket is full, as a part of a wearable package including the actuators.

4.3 Actuator Requirements

4.3.1 For Discrete Event Sensory Control Feedback

To implement a feedback system imitating the DESC scheme, a discrete pulse of stimuli could be used. The time from sending a signal to a perceptible activation should be small $\tilde{1}0$ ms. The configurability of the signal is of less importance, as the information is transmitted through the change in actuator state rather than the state itself.

4.3.2 For Force-level Feedback

To inform the user of different force levels the actuator needs some configurability. Human perception of vibration intensity is linked to booth frequency and amplitude. The ability to disseminate between frequencies diminishes with higher frequencies. Concerning to actuator, this means that at least either frequency or amplitude must controllable, if not both.

4.3.3 For Texture Recognition

If the texture features are divided into categories such as ”smooth, a little rough, and rough”, the actuator requirements are the same as for Force-level Feedback.

If an as accurate as possible reconstruction of the frequency profile recorded at the fingertips is to be reconstructed at the stimulation site, the ability to generate any waveform within a frequency band of $[50 - 400]\,\mathrm{Hz}$, corresponding to the frequency range discernible by the human nervous system.

4.4 Acceptance Requirements for the Complete System

1. Force Sensing
   (a) Be able to detect contact and release events.
   (b) Differentiate between 2-4 force levels.
2. Vibration
   (a) Create discrete pulses of stimuli
   (b) Create stimuli at different intensities.
3. Power Consumption
   (a) Reduce the total power used when gripping an object.
   (b) Have power to run for at least 12 hours a day.
4. Deformation Detection
   (a) Determine digit angles.
   (b) Combine the digit angles and force readings to determine if deformation is occurring.
   (c) Make data regarding deformation available for a possible internal control loop or other applications.

CHAPTER

FIVE

PROPOSED ARCHITECTURE

This chapter includes an overview of the proposed architecture. For a more detailed description of the completed implementation, see chapter 6. The primary goal is for contact force information information to be sensed and transmitted to the user. In addition, deformation detection is to be achieved.

5.1 Force Feedback

The following section outlines the architecture responsible for detecting and informing the user of contact and forces between the fingers of the prosthesis and an object.

5.1.1 Force Sensor

Force sensitive resistors, FSRs, will be attached to the fingers of the prosthesis. Forming a voltage dividing circuit, the value of a second resistor will be read by the ADC of the chosen MCU.

5.1.2 Controlling Unit

The Microchip (previously Atmel) atxMEGA256A3BU offers a satisfying compromise between performance, power usage and price. The MCU has the necessary IO and the compute power required. Using the AVR xplained series of evaluation boards allows for quick prototyping. Using a board, however, includes several bloating components and makes embedding the prototype of the system within the prosthesis or its socket unfeasible.

5.1.3 Actuators

To convey information to the user, a set of vibrotactile actuators, with a one-to-one matching between the sensors and the actuators is proposed. The placement of the actuators is less important when vibrotactile stimulation is used. The actuators must be placed such that they stay in contact with the skin during normal use, but removing them must be at least as easy as removing the rest of the prosthetic system.

5.1.4 Algorithm

To convey discrete events, a burst of stimuli from the actuator will suffice. A burst of vibration, rather than running the motors continuously, has the benefit of saving power, but at the cost of the amount of information that can be conveyed. Further testing and evaluation of the system during construction, will determine if the chosen components are suitable for simple bursts of vibration or if force levels are feasible.

5.2 Deformation Detection

The following section outlines the additions to the force feedback system that have to be made to detect object deformation during grasping.

5.2.1 Angle Sensors

To detect a change in relative joint angles, a sensor for each movable joint is required. To attach the angle sensors to the joints without having to disassemble anything or do irreversible changes to the hand, rotary magnetic encoders will be used. For this type of

encoder a magnet, either permanent or electromagnetic, is required. To mount the encoder, either the encoder or the magnet is fastened to the stator while the other is fastened to the rotor such that the rotation in question will cause a relative, concentric rotation between the two, with the same speed and direction as the rotation in question.

5.2.2 Algorithm

To determine if an object held is being deformed, a combination of contact measurements and joint angles will be used. Whenever two opposing fingers are in contact simultaneously and the finger digits are still moving above some threshold, the system will report object deformation.

Deformation will be classified into two types depending on which pair of fingers involved. A deformation of the first type will be caused by the index finger and thumb, and will be detected by all encoders and the force sensors placed on those fingers. The second deformation type will be cause by the thumb and middle finger. Since there is no space for magnetic encoders on the middle finger, only the encoders placed on the thumb will be used in for this class.

5.3 Software Architecture

The system is implemented on an Atmel/Microchip MCU running no operating system. The program code is written in C, and uses drivers and libraries provided from Microchips Advanced Software Framework. The program runs as a ”big while loop”, where timing interrupts generated from timer counter registers determine what is to be done next.

CHAPTER

SIX

IMPLEMENTATION

The following chapter describes how the hardware was implemented as well as the software. For pictures of the hardware, see Appendix B.

6.1 List of Components

- Interlink Electronics FSR 400.
- Microchip/Atmel XMEGA-A3BU Xplained Evaluation kit for the ATXMEGA256A3BU 16-bit MCU.
- ams AS5413 rotary magnetic encoders.
- Texas Instruments DRV2605L haptic motor drivers.
- Jinlong Machinery & Electronics G0832012 LRA type coin motor.
- Misc resistors, capacitors and diodes. See schematics for values.

6.2 Implementation of Hardware

The following section describes the work done create working hardware and to adapt the prosthesis lab to the Hy5 hand.

6.2.1 Powering the Hy5 Hand

The prosthesis setup present at NTNU was not able to deliver sufficient power to the Hy5 hand. This was especially noticeable when changing from a closing to a opening state, as running both the electric motor as well as operating the solenoid based valves would draw too much current from the battery pack, leading to a voltage drop which in turn sent the hand into a standby mode.

The first attempt at solving the power issue was returning the hand to Hy5 for a software update. Proving unsuccessful, an external power supply was connected to allow for a sufficient amount of current to the hand. This was enough for a while, but a suspected bad connection between the hand and quick connect at the lab as well as long cables running from the power supply to the hand created a unstable and unpredictable hand. Therefore, a new coupling between the hand and power and control signal as well as a shortening of the power cables from around 1m to 5cm, was put in place. This finally solved the connectivity and power issues experienced.

6.2.2 Construction

After ordering parts, testing and familiarisation with the components could be done. Setting up the MCU to measure the FSR through the on-board ADC was the first undertaking. Then, connecting the motor-drivers to the MCU and to the actuators was done. Here, a ordering error made it necessary to convert the package size of the IC's to a larger one more suited for prototyping and use with a breadboard. This was done by soldering the small IC to a conversion PCB. Another problem with the chosen motor-drivers was their identical and non configurable I2C addresses. This was solved though use of resistors, diodes and IO-pins from the MCU. The resulting solution forces the data line of the non selected motor-drivers high when a transmission is taking place to a selected driver. This solution was preferred over controlling the chip select pin of the drivers to allow the actuators to run continuously and independently of each other.

A similar size error was made when ordering the magnetic encoders, requiring the same size conversion as with the motor drivers. The encoders ordered also operate at a 5V logic level, whereas the MCU operates at 3.3V. To overcome this, and to save on the amount of cabling required, the PWM output of the encoders was chosen. This was then doubly low pass filtered and run through a voltage divider before being read at the MCU ADC. Logic level converters could have been used, but were not known of by the author at the time.

6.2.3 Structure of Electronics

The following section will explain the structure of the electronics of the system.

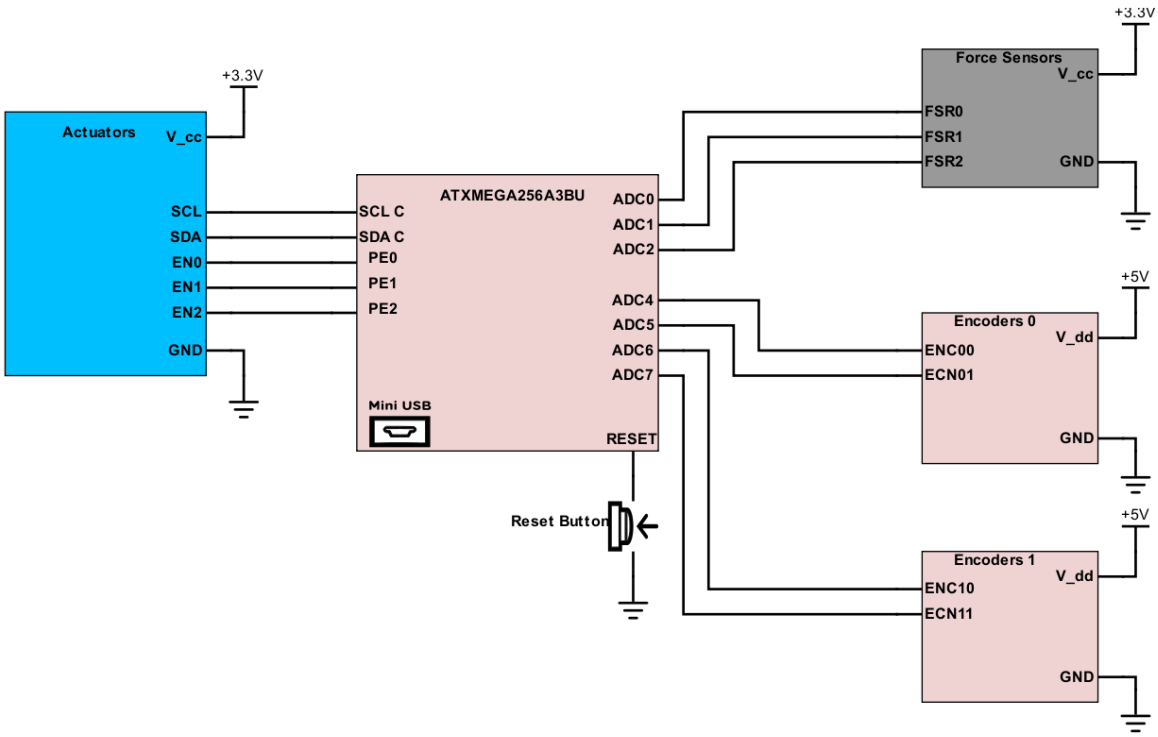

Figure 6.1: Schematic overview of the electronic hardware of the feedback system.

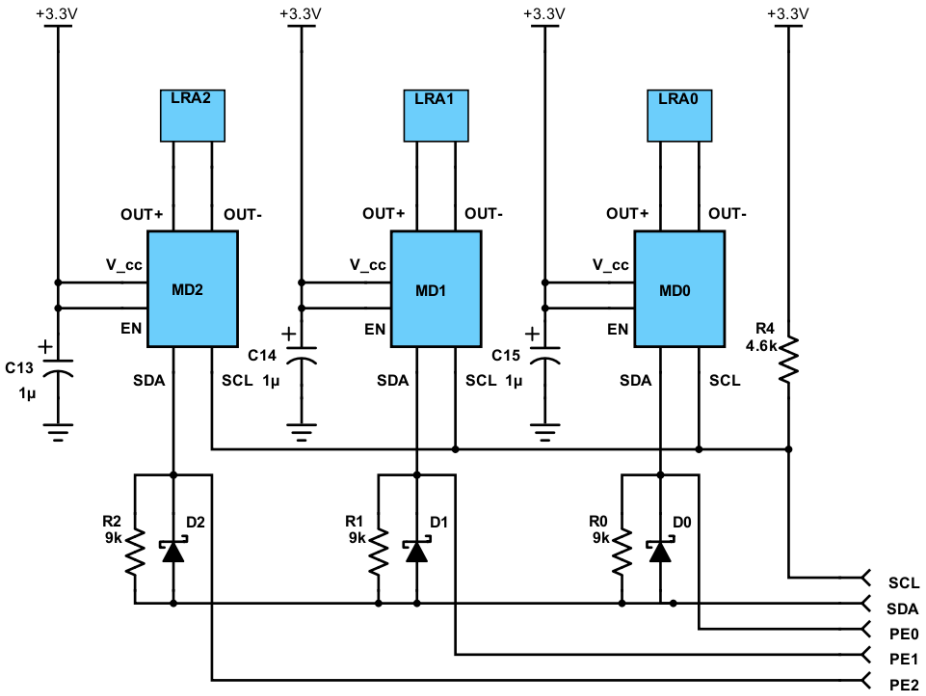

Figure 6.2: Schematic overview of the motor drivers (Texas Instruments DRV2605) and LRA (Jinlong Machinery & Electronics G0832012). R0, R1, R2, D0, D1 and D2 form the solution to the I2C address clash mentioned in 6.2.2.

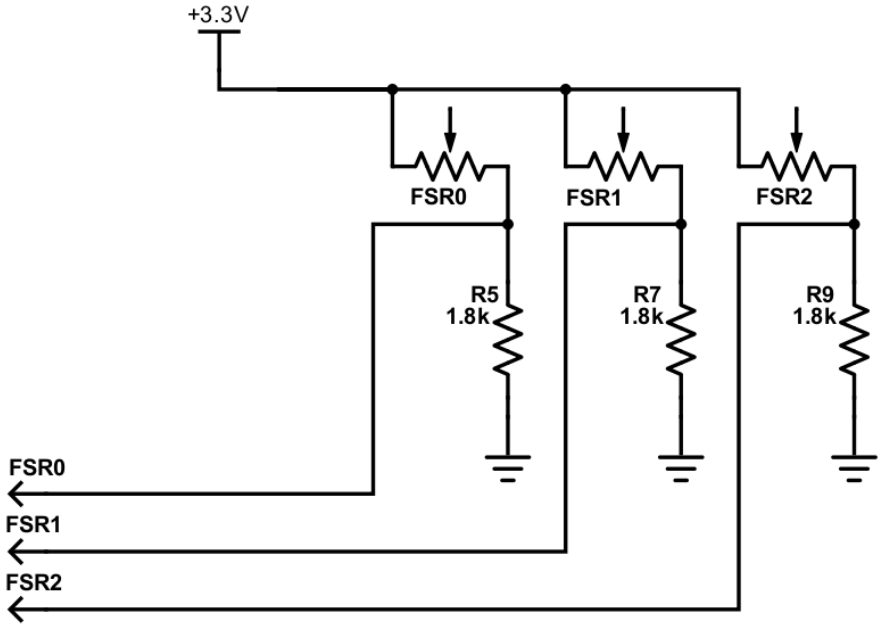

Figure 6.3: Schematic overview of the FSR force sensors (Interlink Electronics FSR400).

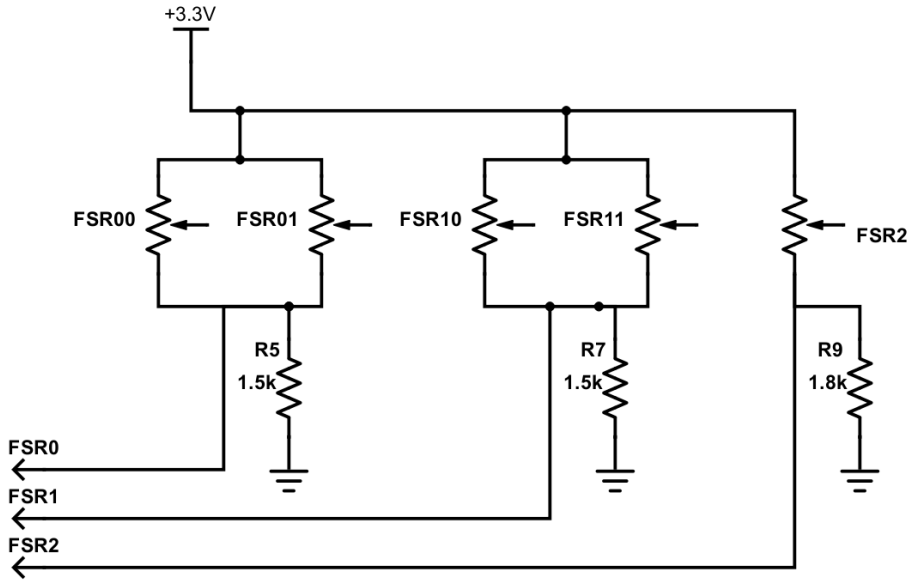

Figure 6.4: Schematic overview of the FSR force sensors (Interlink Electronics FSR400) after extra sensors were added to the index and middle fingers to increase the active area of the sensors.

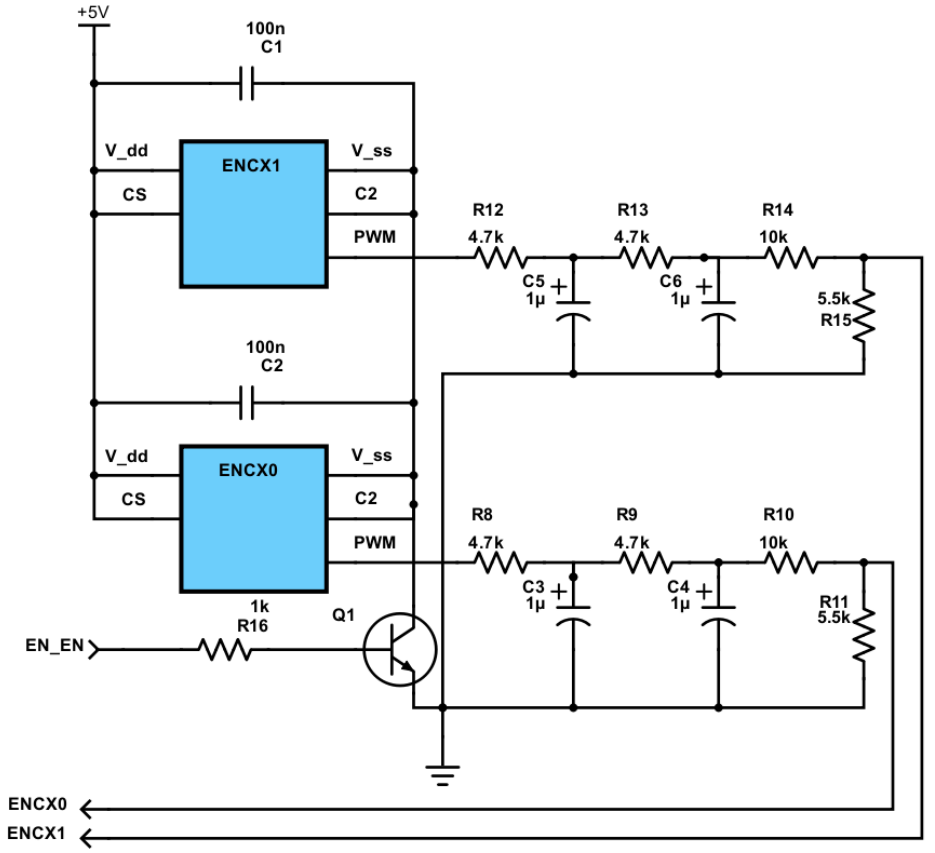

Figure 6.5: Schematic overview of one of the two encoder sets placed on the finger joints of the Hy5 hand (ams AS5134-ZSST). Note that Q1 and R16 represent a shared transistor resistor pair for both the encoder sets and thus power is controlled for all the encoders simultaneously.

6.2.4 Armband for Vibrotactile Actuators

To communicate the vibrations to the user, an armband was created. The armband consists of two layers of elastic fabric sown together. Between these two layers, the actuators and their cables were fastened using an adhesive (super glue) for the actuators, and bent staples for the cables. The cables were fastened in such a way as to relieve the strain on the soldered contact between the cables and the actuators. To allow for some adaptability and easy of donning, the ends of the armband include hook-and-loop (a generic version of Velcro) strips. The distance between the actuators was decided to be 10 cm. This created an even spacing around an upper arm used as a base measurement. Each actuator requires

two wires, OUT+ and OUT- from the motor drivers. These were wrapped in a rubber coating to improve cosmetics and the strength of the cables.

When finished, the armband was tested. It was quickly found that it was difficult to tell which actuator was active, especially when several were running. To create a better haptic rendering on the skin, a hard plastic was cut into circular shapes slightly larger in diameter than the bottom of the LRAs. Holes were cut in the armband and the plastic shapes were glued to the actuator and the armband was resealed.

After testing the armband, as described in section 7.3, a second variant of the armband was designed and implemented. In an attempt to better the ability to discern between amplitudes as well as to be able to tell which actuator was running, housings for the actuators were designed and 3D printed. These were be fastened such that a hard and equal piece of hardened resin would protrude from the armband and press deeper onto the skin. To aid with the tightening of the armband during donning, a zip-tie was fastened to one end such that the other end could be passed through and the armband tightened before securing it using hook-and-loop. Subjective observations also indicated that actuators placed on the medial parts of the arm were felt more clearly. Therefore the actuators and their housings were placed such that their placement on the arm would be more on the medial side of the upper arm than the lateral, i.e the actuator tops were facing the torso. A longer and more flexible cable was also used to allow for more ease of use during testing.

6.2.5 Sensor Mounting on Hy5 Hand

Force Sensors

The FSR sensors were placed on the fingers of the prosthesis. The exact sensor placement was determined by observing where the fingers would contact objects during gripping and holding. The sensors were delivered with double sided tape and this was used to adhere the sensors to the fingers. As per the integration guide for the sensors Electronics (2019). the fingers were flattened to create a better surface for the sensors. To protect the sensors, solder and cabling, and to emulate having a cosmetic glove, a patch of prosthesis glove material was glued to the fingers to cover the sensor and some of the cabling. To read the FSR correctly, and to be within the specified voltage range of the MCU ADC, set at $V_{ref} = V_{cc}/1.6 = 2\text{V}$ the voltage dividing resistor in series with the FSR needs a resistance such that $V_{Rmax} \leq \frac{V_{cc}}{1.6} - \Delta V$ where $\Delta V \approx 0.05 \cdot V_{ref} = 0.1\text{V}$. For the resistor FSR series connection, the minimum value of the resistor is given by $R = \frac{R_{FSR}V_R}{V_{cc}-V_R}$, to

stay within the $1.9\mathrm{V}$ of the ADC. For an FSR saturating at $R_{FSR} = 1k\Omega$, the resistor value is a follows:

$$R = \frac{1\mathrm{k}\Omega 1.9\mathrm{V}}{3.3\mathrm{V} - 1.9\mathrm{V}} = 1.4\mathrm{k}\Omega$$

A similar sensor configuration was also used for the thumb, but with a resistor, R9 in figure 6.4 of $1.8\mathrm{k}\Omega$. This increase in resistance was done so as to increase the sensitivity of the sensor in lower force ranges to better sense first contact. This potential increase in the voltage applied to the ADC-pin is still within the range specified by the MCU-data-sheet.

For a saturation of $R_{FSR} = 1.7\mathrm{k}\Omega$ the resistor value is as follows:

$$R = \frac{1.7\mathrm{k}\Omega 1.9\mathrm{V}}{3.3\mathrm{V} - 1.9\mathrm{V}} = 2.3\mathrm{k}\Omega$$

The sensors active area was assessed by squeezing the fingertips and observing when a touch was detected. The area was found to be a circle with $r \approx 0.5\mathrm{cm}$. During preliminary testing it was found that the sensitive area was insufficient to detect first contact with an object during the closing of the hand, even when the sensor was covered with a force transducing material. To increase the sensitive area of the fingers, a second sensor was placed on both the middle and index fingers. These were then coupled in parallel and fed into the original voltage divider circuit. The two different setups can be seen in figures 6.3 and 6.4.

The longer legged sensor saturates at $R_{satl} = 1.7\mathrm{k}\Omega$, while the shorter legged sensor saturates at $R_{sats} = 1\mathrm{k}\Omega$. If both sensors were to saturate at the same time, the resulting resistance would be $R_{eq} = \frac{R_{satl} \cdot R_{sat_s}}{R_{satl} + R_{sat_s}} = 630\Omega$. In this configuration, the resistor in the voltage dividing circuit would need the following value:

$$R = \frac{0.63\mathrm{k}\Omega 1.9\mathrm{V}}{3.3\mathrm{V} - 1.9\mathrm{V}} = 0.86\mathrm{k}\Omega$$

For this configuration, the resistor value was again increased to heighten the sensitivity of the sensor. As can be seen in figure 6.4, $\mathrm{R5} = \mathrm{R7} = 1.5\mathrm{k}\Omega$, which could result in

a maximum voltage $V_{adc} = 2.7\text{V}$. This would saturate the ADC, but was necessary to achieve touch sensitivity across the finger tips.

6.2.6 Encoders

To measure the angle of the joints of the hand, the magnetic encoders (ams AS5134-ZSST), were used, see figure 6.5 for schematic. Their operation is based on rotating a magnet relative to the Hall-effect probe within the sensor. Therefore, one of the two components needed to be placed on the previous link of the finger, and the next on the link with the associated angle. Both components needed to be placed such that the magnets centre of mass, and the centre of the Hall-effect probe were co-axial to the direction of rotation of the finger joint. To achieve this, two approaches were taken.

For the distal digit, the encoder PCB was fastened to the removable plastic finger tip, which also contains the force sensor. Using a drill, a hole was made in the side walls of the fingertip as well as on the PCB. Using these holes, a screw, plastic washer and three nuts, the encoders were fastened to the fingertip. The magnets were fastened to screws holding the finger digit in place using both electrical tape, as well as double sided tape. The fastening of the PCB to the finger digit was such that the magnet and IC overlapped and the encoder would rotate over the magnet when the digit moved. Care was taken to place the magnet in such an orientation as to ensure that the zero angle of the encoder was outside the movement range of the digit, to prevent the measured value from jumping from a max value to a min value or vice versa.

For the more proximal joint, no easily modifiable part of the hand was available. Therefore, extra standoffs for the encoder PCBs were 3D printed. Each standoff and PCB was fastened together using a bolt, nut, washer and adhesive. The modified encoders were then fastened to the hand using a hot glue gun, as the components hot glued to the hand can be removed and cleaned without damaging the hand or components.

6.3 Software

The following section describes the software as implemented. The main application is a ”big while loop” where every action runs to completion. The after all actions are complete the system is put to sleep. Periodic timing interrupts wakes the MCU from Structure of modules with function names and attributes is shown as a class diagram. The force sensor module has available in it code base functions for creating and outputting discrete force levels rather than a raw digital value. However, the state machine implemented as a part of the finished system is only based around contact or not contact. If in the future more force information is necessary, such functionality exists.

A series of sequence diagrams show the flow of operation when the system is running. Figure 6.6 shows a class diagram for the modules created as a part of this thesis and their main dependencies. Figure 6.8 shows the start up routine completed at each reset of the MCU. For the shown start up, no FSR calibration is done, and either data stored or default values are used to define the force levels. Figure 6.8 shows the FSR calibration routine with prompts printed to the evaluation board screen. Figure 6.9 shows a state diagram for the state machine implemented as a big while loop responsible for the primary application. Transitions from the sleep state is triggered by timing interrupts. For a more detailed look at the code and modules, see Appendix A or the project code files.

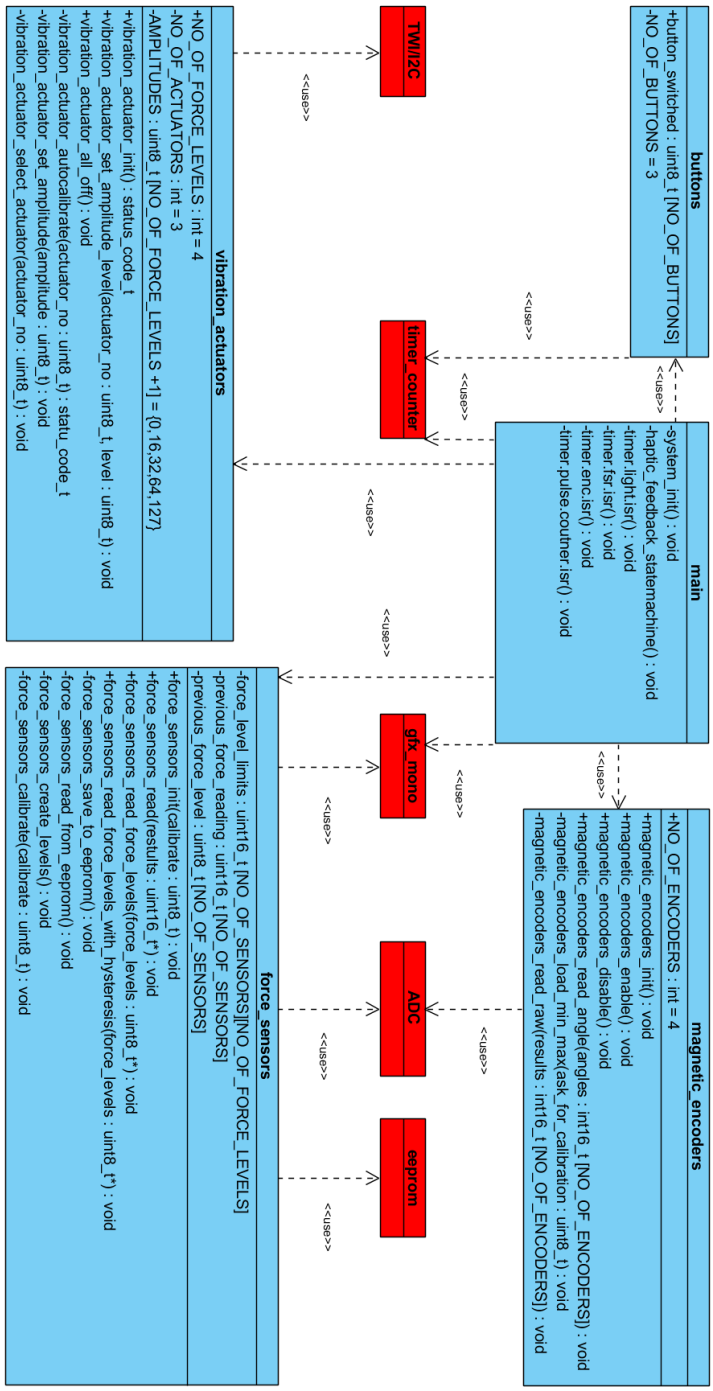

Figure 6.6: Class diagram showing the structure of the developed code. Class names correspond to names of header and C files, see appendix A. Red classes are modules provided through ASF

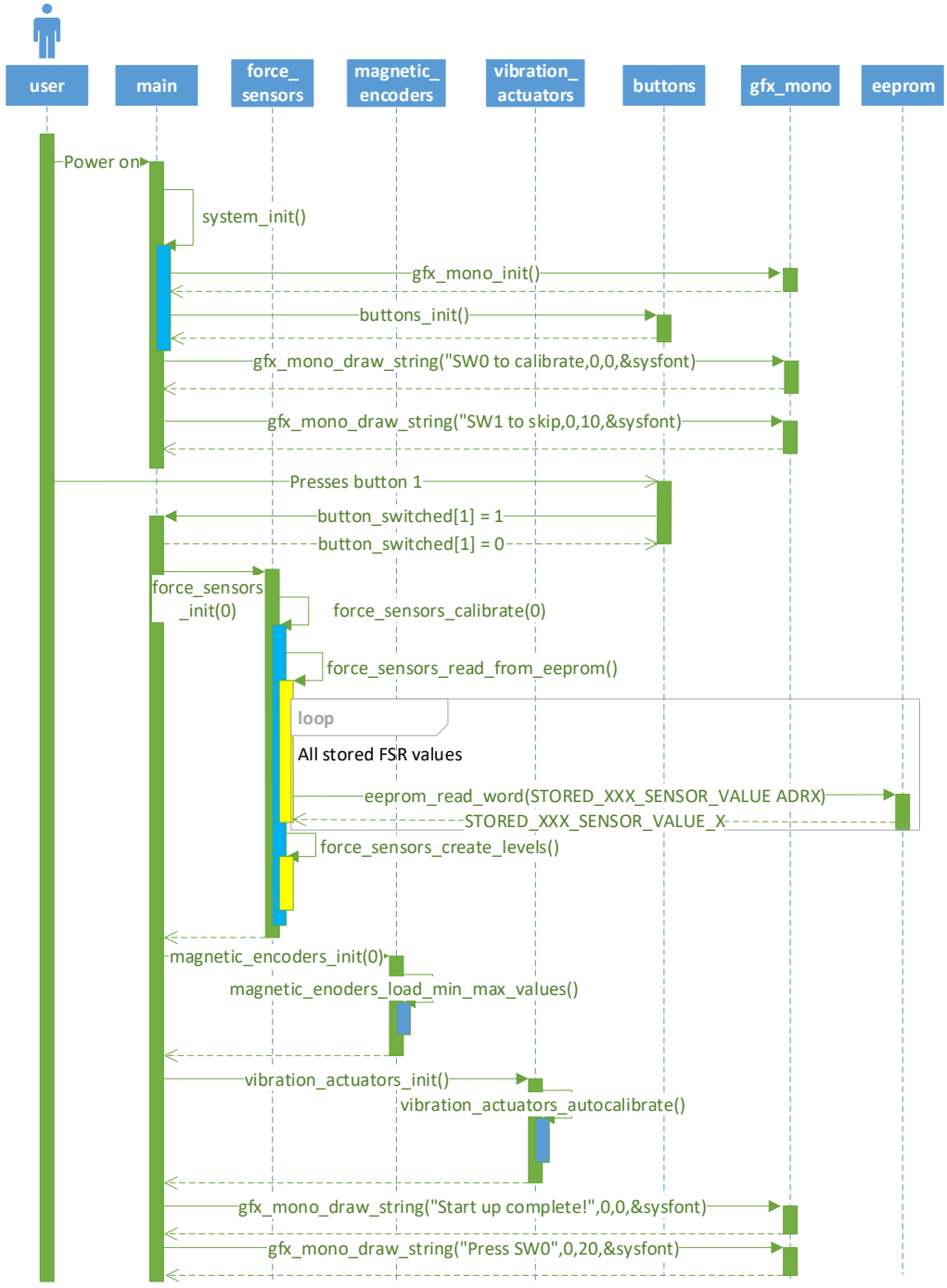

Figure 6.7: Sequence of system start-up with user opting not to calibrate sensors, but rely on data stored from a previous calibration. If there is no stored data, default values are used.

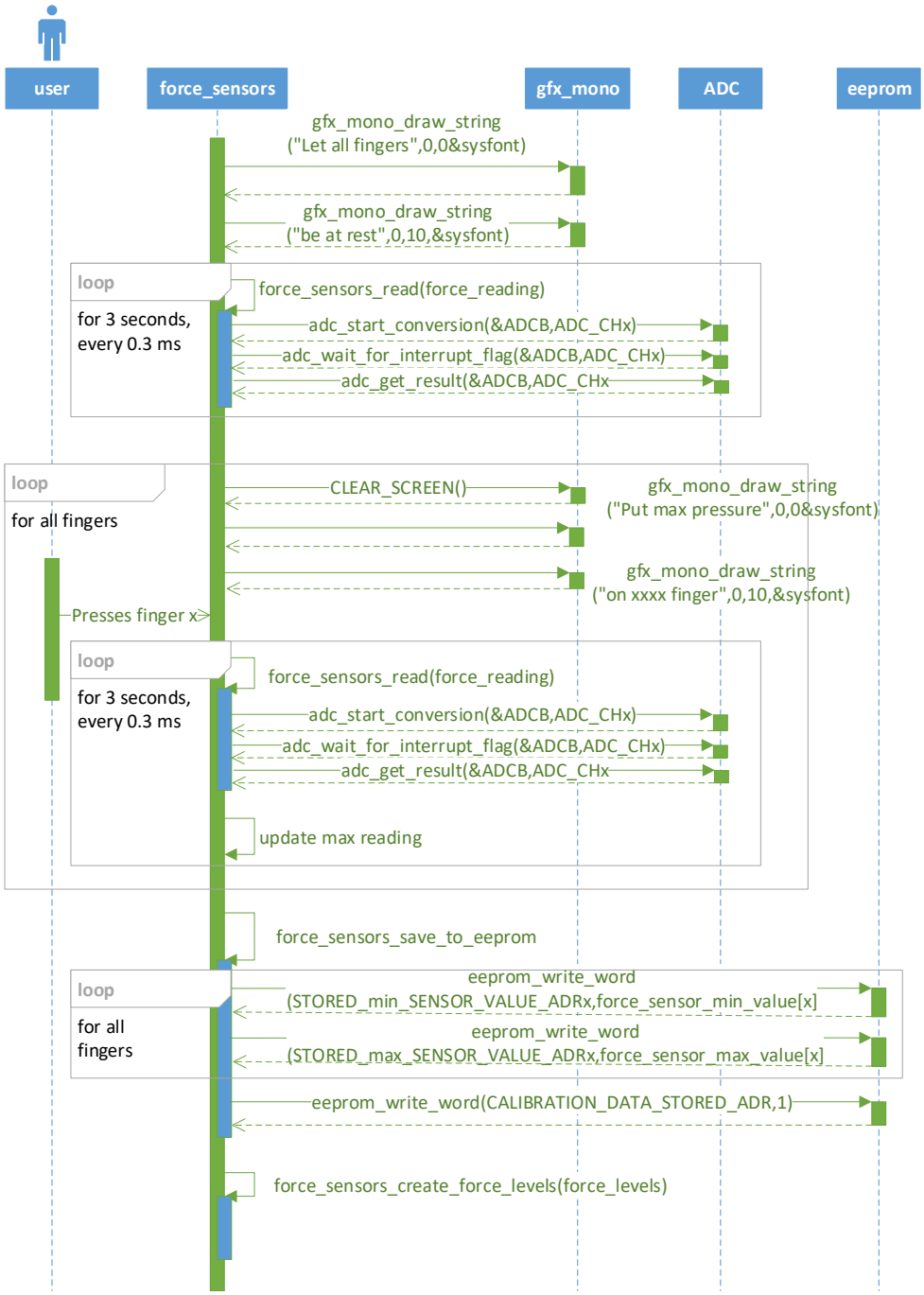

Figure 6.8: Sequence of FSR calibration routine.

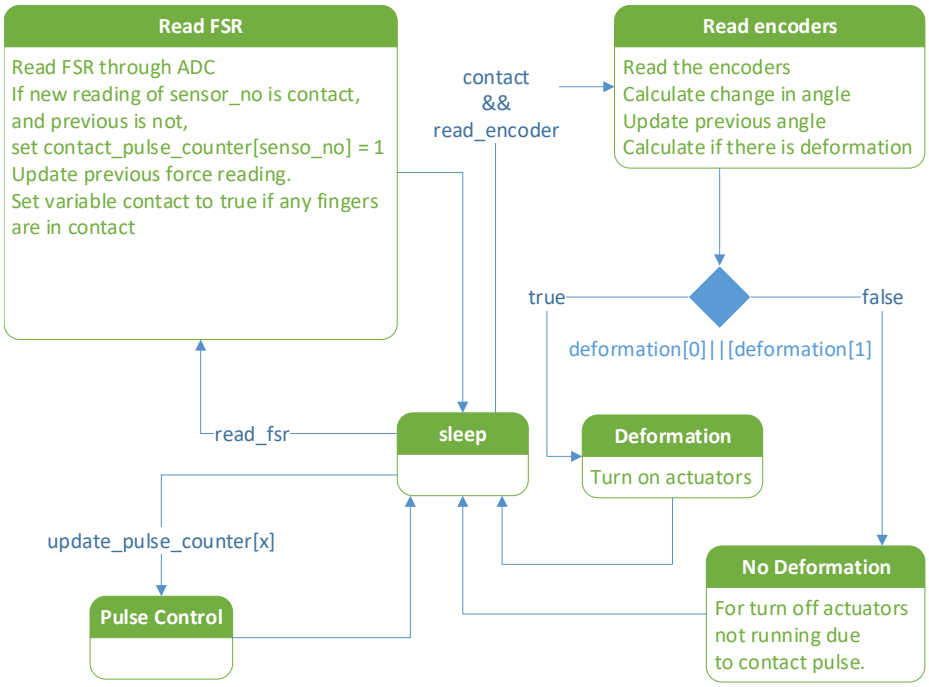

Figure 6.9: State diagram showing the haptic_feedback_state_machine responsible for the main application. Pulse control block is shown in figure 6.10.

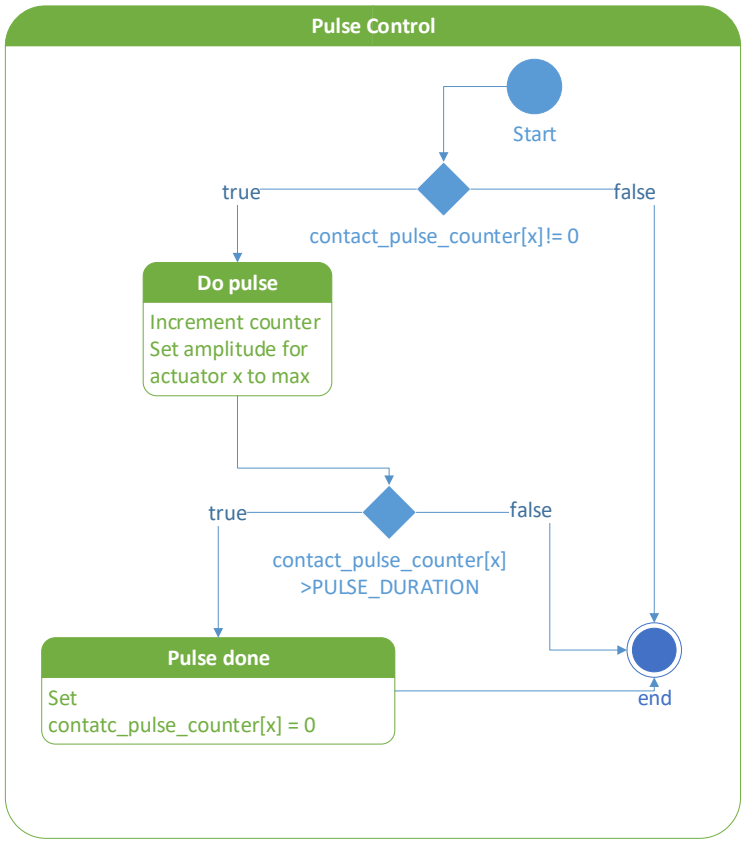

Figure 6.10: State diagram showing the Pulse Control block from figure 6.9.

CHAPTER

SEVEN

TEST METHODOLOGY

The following chapter outlines the methods used for the tests performed. The results can be found in chapter 8.

7.1 LRA Compatibility with EMG

The Hy5 hand is controlled via EMG sensors placed on the residual limb of the prosthesis user. These pick up the changing electric fields that propagates as a muscle contracts. To verify the chosen actuators compatibility with EMG sensors, a simple test was conducted. The test consisted of reading the EMG signal coming from a sensor placed on an arm in a position similar to where a sensor embedded within a prosthetic socket would be. The signal was recorded under three different conditions. First, a base reading with little to no muscle contraction and no LRA running in the room. A second, with little to no muscle contraction, with an LRA running at maximum amplitude being moved around the sensor to verify that their relative orientation was of no importance. The third case was a muscle contraction with no LRA present to have another point of comparison.

7.2 Force Sensitivity Testing

To determine the effects of covering the FSR with different materials, a variable and measurable weight was placed in on the the sensor under three conditions, and the voltage over a resistor, $R = 9.85\text{k}\Omega$, coupled in series with the FSR was measured. The three conditions were: uncovered, covered by a thin piece of rubber latex cut from a dish-washing glove and covered by a thicker piece of material cut from the same material used for cosmetic gloves typically worn outside a prosthetic hand.

In order to vary the force pressed down against the sensor, a modified funnel was used. The funnel was modified so that the bottom would no longer allow pieces of solid matter to fall through. The tip used to make the funnel tight had a small circular extrusion with a diameter closely matched to that of the active area of the FSR. The weight of the tipped funnel was measured, and to change the weight pressing down on the sensor a weighed amount of dry rice was added to the bowl of the funnel. The weight used was a kitchen weight with a resolution of 1g. Rice was chosen over water as spilling water over the lab would be catastrophic, while spilling dry rice would be an inconvenience, and the size of grains of rice still allows for a greater resolution than achievable by the weight used.

However, even when creating a more stable stand than a funnel and knob, the measuring process yielded unrepeatable results, and was discarded. A new method was devised after consulting with the technical staff working at the Department of Engineering Cybernetics. There, two dial gauges, one with a resolution of 0-100g and another with 0-1000g were made available. A clamping tool was also provided. Using the tip of the dial gauge to press down on the sensor and holding the dial gauge in a fixed position, it was possible to create a controlled and repeatable downward force on the sensor.

The first set of measurements was done with the tip of the gauge pressing directly onto the active sensor area. For the measurement results, see table 8.9. This however broke the sensor by pressing the two layers of the FSR together permanently, ensuring that the resistance of the sensor was always below the open loop characteristic normally displayed by a non actuated FSR. For the remaining test runs, a small piece of hard plastic was cut and ground down to fit the dimensions of the active area of the sensor. This plastic piece, refereed to as a ”block” in the results table, was placed between the tip of the gauge and the sensor, resulting in a lower, but even pressure on the sensor. As described, the sensor was covered with a piece of dish-washing glove material as well as a piece of artificial skin after the uncovered tests were done.

7.3 Vibration Sensation Testing

The following sections describe what tests were done using the setup described and implemented in section 6.2.4.

7.3.1 Minimum Perceivable Amplitude

To determine the feasible amount of force levels that could be conveyed using the current setup, a test was devised. Using one of the actuators at a time, the minimum amplitude easily detectable was sought. This was done by testing the ability to determine when the actuator was turned on. If no vibration was felt, the amplitude was increased by incrementing the value written to the amplitude register in the motor driver chip.

This test was repeated for all three actuators, which were placed almost equidistant from each other within the armband, their distance from each other depending on the level of tightening done when donning the armband.

7.3.2 Minimum Perceivable Difference in Amplitude

To explore how many different levels a user could recognise, another test was needed. This time, for each of the actuators, the difference between the amplitude was varied. Switching between to amplitudes was done, increasing the difference between the two amplitudes until a difference could be reliably felt. This was done for multiple ”base” amplitudes for each actuator.

7.3.3 Discrete Pulse Testing

To test how clearly one could tell which actuator was active, a test where the actuators pulsed for 100ms in random order, was conceived. For the next actuator to pulse, a button had to pressed and after two seconds the next pulse would fire. During the test the subject wore a noise cancelling headset playing music.

As a follow up test, two actuators was activated at the same time for a 100ms pulse. The same setup with a headset and a button press between each pulse was used.

7.4 Power Consumption

While data-sheets provide a good indication of power consumption in many cases, the power usage of the finished subsystems was measured to check the consumption in the actual configuration used. To measure the power consumption, an ammeter was connected in series with the subsystem being tested. The current was then measured in at least two states for each subsystem.

Hy5 recommends their hand be used with a 7.2 V 2000mAh battery, capable of delivering a maximum current of 5A Hy5 (2017). This gives a energy capacity of 14 400 mWh. When running the hand, the power consumption was observed by observing the external power supply.

7.5 Grip Testing

One of the primary goals of the feedback system is to allow users to detect grip contact without relying on their visual or auditory senses. To this end, a test was performed where different objects one might encounter in daily life was grabbed. During testing, the prosthesis was controlled using the slider and button-setup described in section 1.4. To determinate if the time of contract corresponded with when the system was able to detect the onset of contact, the griping sequence was filmed using a mobile phone camera.

The objects in this test varied in shape, size and rigidity. The following list outlines the objects included in the test:

- Water bottle made from a hard plastic.
- Pen.
- Paper cup.
- Empty plastic tomato container.

To signal a contact event, LEDs included on the MCU evaluation board would light up, one LED for each finger. Additionally, the sensor states were written to the LCD screen on the board. Using the LEDs and screen instead of using the feedback system allows for a more quantitative measurement of the time between contact and contact detection.

7.6 Deformation Testing

Similarly to the grip testing in section 7.5, a test to verify that the system can detect deformation was undertaken. Again, the test was filmed using the same camera and LEDs were used to indicate a detected deformation. Deformation was classified into two types depending on which prosthetic fingers were involved.

The objects in this test varied in shape, size and rigidity. The following list outlines the objects included in the test:

- Water bottle made from a hard plastic.
- Paper cup.
- Empty plastic tomato container.

Before the test was undertaken, it was verified that a closing digit movement combined with contact on two opposing finger tips on the prosthesis would result in a reported deformation. This was done by holding the prosthetic finger tips firmly and moving them through their range of motion.

CHAPTER

EIGHT

RESULTS

In this chapter, the results of tests and methods described in the previous chapter are presented.

8.1 Vibration Sensation Testing

Following are the results from the tests regarding the vibrotactile armband.

8.1.1 Single Site Pulse Testing

Following are the result of the first test described in section 7.3.3.

	Run 1		**Run 2**		**Run 3**	
Pulse	*Actuator Running*	*Site Felt*	*Actuator Running*	*Site Felt*	*Actuator Running*	*Site Felt*
1	0	0	1	1	0	0
2	0	0	1	1	1	1
3	1	1	2	2	0	0
4	2	2	1	1	0	0
5	1	1	2	2	0	0
6	0	0	1	1	2	2
7	2	2	1	1	1	1
8	2	2	0	0	0	0
9	1	1	0	0	0	0
10	0	0	0	0	2	2
11	1	1	2	2	1	1
12	2	2	1	1	0	0
13	0	0	1	1	1	1
14	2	2	1	1	2	2
15	0	0	0	0	2	2
16	1	1	1	1	1	1
17	2	2	1	1	1	1
18	0	0	1	1	0	0
19	1	1	2	2	1	1
20	0	0	0	0	2	2

Table 8.1: Table showing the results of the single vibration test for the first arm band. During these trials, a 100% success rate was observed.

	Run 1		**Run 2**		**Run 3**	
Pulse	*Actuator Running*	*Site Felt*	*Actuator Running*	*Site Felt*	*Actuator Running*	*Site Felt*
1	0	0	2	2	0	0
2	2	2	0	0	1	1
3	2	2	1	1	2	2
4	2	2	2	2	1	1
5	2	2	2	2	0	0
6	0	0	0	0	0	0
7	2	2	2	2	1	1
8	1	1	2	2	0	0
9	0	0	0	0	0	0
10	2	2	1	1	2	2
11	2	2	2	2	2	2
12	1	1	1	1	0	0
13	1	1	1	1	1	1
14	0	0	2	2	0	0
15	0	0	2	2	0	0
16	1	1	1	1	1	1
17	2	2	0	0	1	1
18	0	0	2	2	0	0
19	0	0	1	1	2	2
20	1	1	0	0	0	0

Table 8.2: Table showing the results of the single vibration test for the second arm band. During these trials, a 100% success rate was observed.

During all three tests, for both of the armbands, the correct actuator was identified in 100% of the cases.

8.1.2 Dual Site Pulse Testing

The following tables show the results of the second test described in section 7.3.3. Table 8.3 shows the results when the first iteration of the armband was used. Table 8.4 shows the results when the second iteration of the armband was used.

	Run 1		**Run 2**		**Run 3**	
Pulse	*Actuators Running*	*Sites Felt*	*Actuators Running*	*Sites Felt*	*Actuators Running*	*Sites Felt*
1	02	02	01	02	12	12
2	12	12	02	02	01	01
3	02	01	02	02	12	12
4	01	01	01	01	01	01
5	02	02	01	01	01	01
6	12	12	02	02	02	02
7	01	02	01	01	01	01
8	02	02	12	12	12	12
9	02	02	01	01	12	12
10	02	02	02	12	12	12
11	12	02	12	12	12	12
12	01	01	01	01	02	02
13	02	02	02	02	01	01
14	12	12	02	02	02	12
15	12	12	01	01	12	12
16	01	01	02	02	02	12
17	02	02	02	02	01	01
18	01	01	12	01	02	12
19	02	02	02	12	12	12
20	12	12	01	01	01	01

Table 8.3: Table showing the results of the dual vibration test performed on the first armband. Mismatches are indicated by dark grey fields

	Run 1		**Run 2**		**Run 3**	
Pulse	*Actuators Running*	*Sites Felt*	*Actuators Running*	*Sites Felt*	*Actuators Running*	*Sites Felt*
1	01	01	02	01	01	01
2	01	01	12	12	12	12
3	02	02	02	01	02	01
4	01	01	02	01	02	02
5	02	12	02	01	12	12
6	01	01	01	01	02	02
7	12	12	01	01	02	12
8	12	12	12	01	12	12
9	01	01	02	02	01	12
10	12	12	02	01	02	12
11	01	01	02	01	02	02
12	01	12	01	01	12	12
13	02	02	02	02	02	02
14	01	01	12	12	01	01
15	01	01	02	01	02	12
16	01	12	02	02	01	01
17	12	12	02	02	01	01
18	01	01	12	12	02	01
19	12	12	12	12	02	02
20	02	01	01	01	01	01

Table 8.4: Table showing the results of the dual vibration test performed on the second armband. Mismatches are indicated by dark grey fields.

Subjective observations were that actuators placed on the medial part of the arm felt sharper and more spatially accurate. The sensation of actuators placed in that area also had a more tingling quality, and the felt effects persisted for a little while even after the actuator had been turned off.

8.1.3 Vibration Amplitude Testing

The following two tables are the results from the amplitude test described in sections 7.3.1 and 7.3.2.

Actuator	*Run 1*	*Run 2*	*Run 3*
0	20	18	20
1	15	13	12
2	23	25	25

Table 8.5: Results of the minimum detectable amplitude, as described in section 7.3.1, using the first armband.

Actuator	*Run 1*	*Run 2*	*Run 3*
0	10	12	11
1	20	15	18
2	12	15	12

Table 8.6: Results of the minimum detectable amplitude, as described in section 7.3.1, using the second armband.

Actuator	**Base Amplitude**	*Minimum Difference 1*	*Minimum Difference 2*
0	20	20	20
	50	*Inf*	*Inf*
	80	*Inf*	*Inf*
1	15	15	15
	45	30	25
	80	*Inf*	*Inf*
2	25	15	13
	60	*Inf*	*Inf*
	90	*Inf*	*Inf*

Table 8.7: Results of the test performed to determine the minimum discernible amplitude, as described in section 7.3.2 using the first armband. The same test was run twice.

Actuator	**Base Amplitude 1**	*Minimum Difference 1*	**Base Amplitude 2**	*Minimum Difference 2*
0	10	15	15	15
	25	45	30	40
	45	Inf	40	Inf
1	15	20	20	15
	35	30	35	20
	65	Inf	55	Inf
2	15	15	15	15
	30	25	30	30
	55	Inf	60	Inf

Table 8.8: Results of the test performed to determine the minimum discernible amplitude, as described in section 7.3.2 using the second armband. The test was run two times, but with different base amplitudes.

8.2 FSR response

The following table shows the measurements taken during the FSR test described in section 7.2. The following graphs show the FSR resistance values.

	V_R[V]			
Weight[g]	**No Cover**	**Only Block**	**Block and Glove**	**Block and Artificial Skin**
10	0.08	0	0	0
20	0.3	0	0	0
40	0.56	0	0.1	0
60	0.64	0	0.70	0.1
80	0.68	0	0.83	0.43
125	0.70	0.22	1.4	1.0
150	0.78	0.45	1.6	1.2
300	0.98	1.5	2,0	2.0
400	N/A	1.7	2.2	2.1
500	N/A	2.0	2.2	2.2
600	N/A	2.1	2.3	2.3
800	N/A	2.2	2.4	2.4
1000	N/A	2.3	2.4	2.4

Table 8.9: Table showing the results of the sensitivity test described in section 7.2.

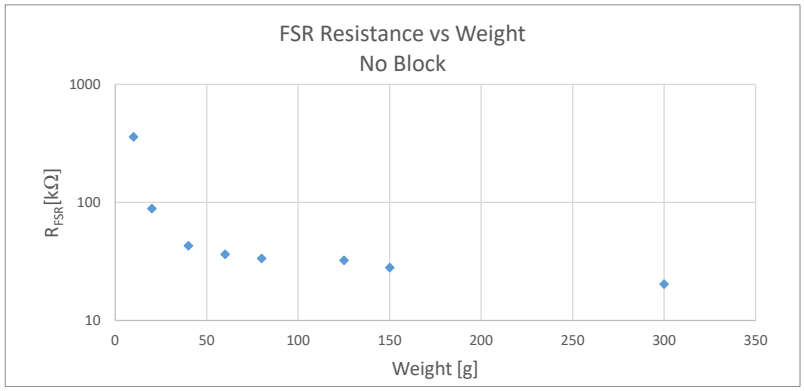

Figure 8.1: Graph showing FSR resistance as a function of weight applied to a small point, as described in section 7.2.

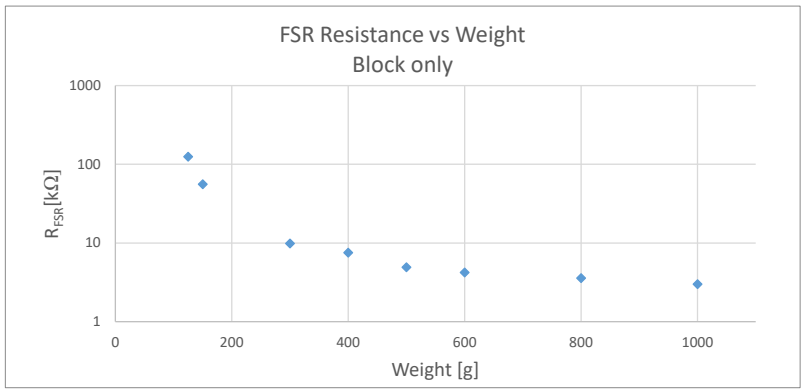

Figure 8.2: Graph showing FSR resistance as function of weight applied evenly over the active area of the sensor, as described in section 7.2.

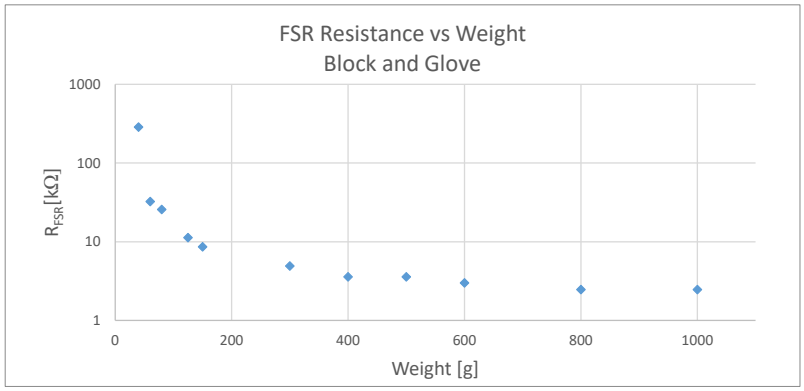

Figure 8.3: Graph showing FSR resistance as function of weight applied evenly over the active area of the sensor when covered by a piece of a dish-washing glove, as described in section 7.2.

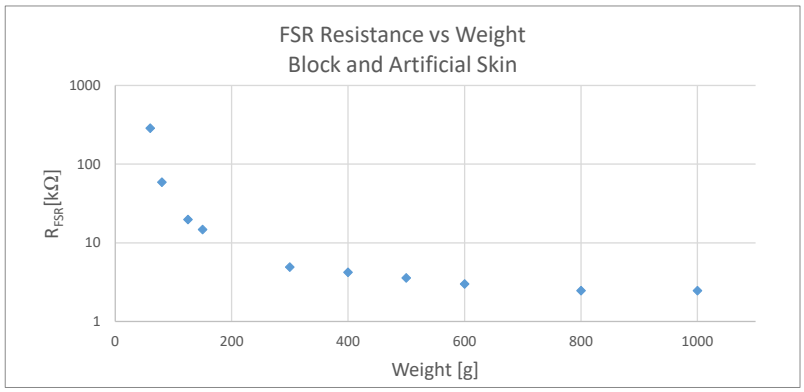

Figure 8.4: Graph showing FSR resistance as function of weight applied evenly over the active area of the sensor when covered by a piece of a artificial skin, as described in section 7.2.

8.3 Cost

The following section presents the monetary cost of the system. For the MCU, the cost of the MCU, not the board, is presented. The cost of cables, transistors, capacitors and diodes is excluded. The cost of assembly and integration is excluded. The cost of extra materials used in prototyping such as glue, tape and breadboards is excluded. The price of an optional custom FSR solution is not presented here.

Component Type	**Component Name**	Price pr Item	*Number Needed*	*Subtotal*
MCU	ATxmegaA3BU	60	1	60
Motordriver	DRV2605L	31	3	93
LRA	G0832012	27	3	81
Force Sensor	Interlink FSR 400	84	5	420
Magnetic Encoder	AS5134	66	4	264
Magnet	Small magnet	3	4	12
Encoder Housing		2	3	6
Encoder Standoff		3	2	6
Elasic Band		50	1	50
Total				992

Table 8.10: Table showing the cost of components, excluding passives such as resistors, capacitors, diodes and wires. All prices except for 3D printing and the elastic band is collected from Digikey.no. All prices are in NOK.

8.4 Power Consumption

The following table shows the power consumption of the subsystems of the feedback system, as described in 7.4.

Subsystem	State	Current [mA]	Voltage [V]	Power [mW]	Comment
Motor drivers and actuators	All actuators running 100%	156	3.3	515	Right after start-up
Motor drivers and actuators	All actuators running 100%	70	3.3	230	After squeezing the actuators
Motor drivers and actuators	All actuators off	7.5	3.3	25	
FSR circuits	All sensors measuring 0	0	3.3	0	
FSR circuits	Index finger saturated	1.3	3.3	4.3	
FSR circuits	Middle finger saturated	1.3	3.3	4.3	
FSR circuits	Thumb saturated	1	3.3	3.3	
Encoders and filters	Powered down	0.55	5	2.8	
Encders and filters	Powered up, moved around and sampled	58	5	290	
MCU	Running Haptic Feedback state machine	22	3.3	73	

Table 8.11: Test of subsystem power consumption under different conditions.

This results in an idle power consumption of $P_{idle} = 390\mathrm{mW}$ with all sensors powered on, $P_{idle} = 100\mathrm{mW}$ with the encoders disabled, and a maximum power draw of $P_{max} = 880\mathrm{mW}$.

For each discrete pulse of duration $100\mathrm{ms}$, which was the period of all pulse tests, by all actuators at once, the energy used by actuators and drivers would amount to $W_{Pulse} = 52\mathbf{mJ}$. Assuming the closing of the hand takes 1 second and is drawing $4\mathbf{A}$ at $7.2\mathrm{V}$, the

energy spent is around 29J. Adding one pulse to the closing operation increases the power usage by less than 0.2%.

Running the MCU and other peripherals with the encoders in a powered down state, for a 12 hour day, the system would use less than 9% of the battery capacity. With the encoders enabled and running, the system would use 33%. These percentages are valid provided a battery with the specifications recommended by Hy5 is used.

8.5 LRA compatibility with EMG

The following graphs show the output from one of the LabView programs described in section 1.4. The three figures show the EMG signal with no LRA present and no contraction, EMG with LRA present and running at 100%, and for context, a muscle contraction is shown in the final image.

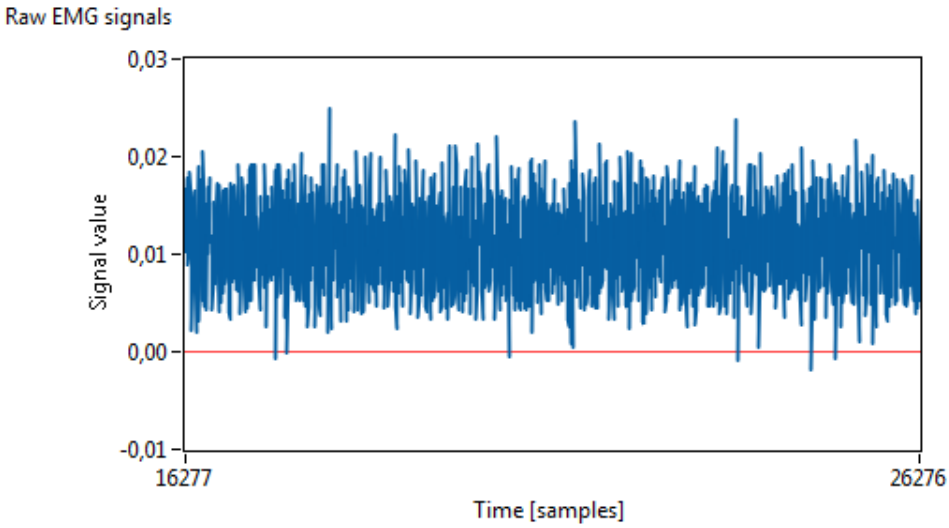

Figure 8.5: Raw EMG signals with no LRA present.

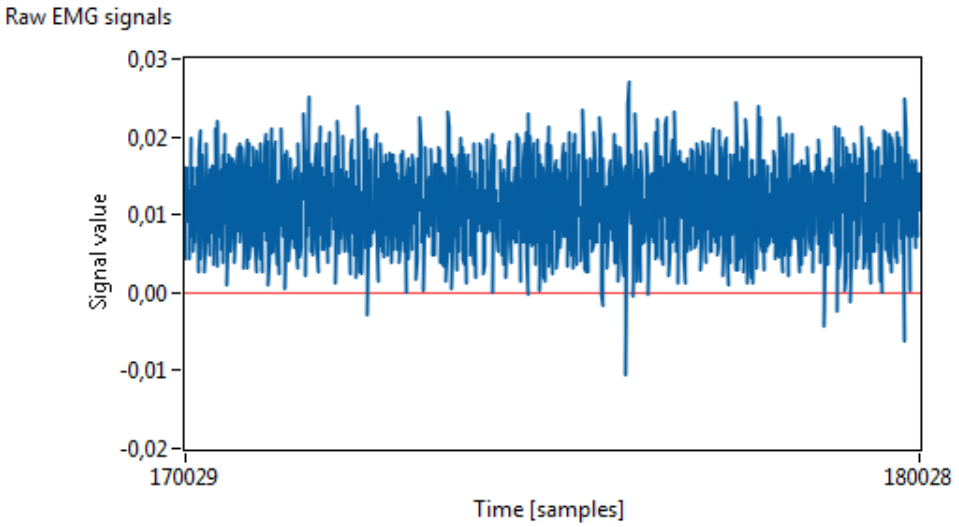

Figure 8.6: Raw EMG signals with LRA present, running at maximum amplitude.

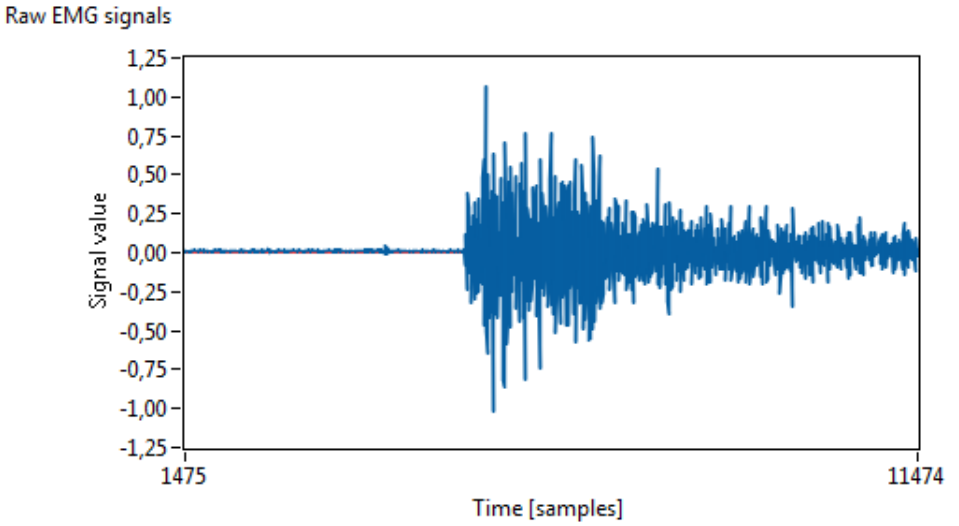

Figure 8.7: Raw EMG signals with a strong muscle contraction starting close to the middle of the plot.

8.6 Grip Testing

The following table displays the results from the grip test described in section 7.5. LED0 corresponds to the index finger, LED1 to the middle finger and LED2 to the thumb.

Object Gripped	Success	LED0	LED1	LED2	Comment
Paper cup	No	0	0	0	Object crushed with no detection.
Paper cup	No	0	0	0	Object crushed with no detection.
Plastic container	Partial	0	1	0	After tighetning, index detects object.
Plastic container	Partial	1	1	1	No stable detection achieved. Only detection after some deformation.
Pen	Yes	0	1	1	Pen gripped perpendicular to finger direction. Thumb detects at once, middle finger a little later.
Pen	No	0	1	0	Pen gripped parallel to fingers. Middle finger only after jiggeling the pen.
Pen	No	0	0	0	Pen gripped parallel to fingers. Ends up between middle and index fingers.
Pen	Partial	0	1	0	Index finger detects contact.
Water bottle	Partial	0	1	0	Water bottle gripped such that the ”un senosorised” parts of the thumb and index fingers are in contact.
Water bottle	Yes	0	1	1	No detection at index finger.
Water bottle	No	0	0	0	Water bottle gripped with distal parts of all fingers and is such out of the sensorised parts.

Table 8.12: Results of grip test as described in section 7.5.

8.7 Deformation Detection

The following table displays the results from the deformation test described in section 7.6. LED0 corresponds to the thumb / index finger pair, while LED2 corresponds to the thumb / middle finger pair.

Object Gripped	Success	LED0	LED2	Comment
Paper cup	No	0	0	Object crushed with no detection.
Paper cup	No	0	0	Object crushed with no detection.
Plastic container	No	0	0	Object crushed with no detection
Water bottle	Partial	1	0	When the thumb moved/ slid across the bottle, detection was signaled
Water bottle	Yes	0	0	No deformation, or movement after contact made.

Table 8.13: Results of deformation test as described in section 7.6.

The proof of concept test where the prosthetic fingers were moved manually showed that both types of deformation described in section 5.2.2 were detected when the expected sensory input was present.

CHAPTER

NINE

DISCUSSION

This chapter is a discussion of the results presented in chapter 8 and the implemented system as described in chapter 6.

9.1 LRA Compatibility with EMG

The following section discusses the results presented in section 8.5.Inspecting figures 8.6 and 8.5, no clear difference can be found. If a difference is present, any such interference can be ignored as the both signal amplitudes fall well below the amplitude of even a moderate muscle contraction by a factor of 100. Thus, even when placed in very close proximity to the EMG sensor, the LRA has no disturbing affect on the EMG signal recorded. Therefore it has been confirmed that LRAs are compatible with EMG control.

9.2 Vibration Sensation Testing

The following two section discuss the results of the test performed using the vibrotactile armband presented in section 8.1. Regarding the testing methodology itself, all tests were performed by and on the author. This gave the subject of the tests all information

about timing and the expected number of actuators running, even though which actuator was running was randomised for the pulse testing. This knowledge of timing is especially problematic for the minimum amplitude tests, where anticipating the activation of an actuator could lower the threshold for the lowest amplitude perceivable.

9.2.1 Single Site Pulse Testing

The following section discusses the results presented in section 8.1.1. The correct actuator was identified in all tests and for both armbands. This suggests that both versions of the armband are suitable for discrete event feedback, when only one actuator is active at once.

The different placement of the actuators had no impact on the success rate of the tests. When the second armband was in use, only around 50% of the circumference of the arm was covered. The then covered area was the part of the skin between the two most distant actuators. Therefore, it is reasonable to believe that at least one more actuator could be placed on the surface of the skin along the same circumference. The extra actuator could be paired with and extra force sensor placed on the passive fingers of the Hy5 hand or used to convey some other information regarding the prosthesis.

9.2.2 Dual Site Pulse Testing

The following section discusses the results presented in section 8.1.2. In contrast to the single site test, the dual site test did not yield a 100% success rate. The average success rate for the first armband was 83% while for the second the rate was 70%.

For both armbands, the results from this test suggest that the more actuators are running, the harder it becomes to discern which are active, especially when the actuators are placed in close proximity. While it has been reported that increasing the normal force pressing down on a vibrotactile actuator Motamedi et al. (2017), no performance increase in the dual site test was observed. Although no measurement of the normal force exerted by the armband extrusion onto the skin were made, subjective observations indicated that the tightening mechanism of the second armband did push the housing deeper into the skin than the plastic parts used in the first armband.

One of the goals when making the second armband was to improve the results from the dual test. This was not successful. The fact that both armbands displayed sub-optimal performance, even when the timing and number of actuators being activated was known,

suggests that further work on actuator placement, interface with the skin or other parameters, is required before the armband can be used in situations where more than one actuator is active at a time.

9.2.3 Minimum Perceivable Amplitude

The following section discusses the results presented in section 8.1.3. For both armbands, actuators 1 for the first band and 0 for the second provided the smallest minimum amplitude, suggesting that that part of the skin was most sensitive to vibration. This was on the medial side of the arm, approximately where the biceps rests on the humerus. For the exact location, see appendix B. This is in line with the subjective reports that stimulation in that area felt sharper and more tingly.

A reduction in the minimum amplitude was observed when going from the first to the second armband. This was especially apparent when considering actuator 1's placement from the first armband corresponds to actuator 0's placement from the second armband. For actuator 2, the placement was similar for for both armbands.

This lowering of the minimum perceivable amplitude could be caused by an increase in downwards force pressing the actuator and corresponding housing or piece of plastic further into the skin. The second armband's housing also created a smaller area in contact with the skin, creating vibration in a smaller area.

9.2.4 Minimum Perceivable Difference in Amplitude

The following section discusses the results presented in section 8.1.3. If the actuators are to convey discrete levels of stimulation intensity, for the first armband two non zero levels were feasible. For the second armband three were considered feasible, with the first non zero level placed at the minimum perceivable, the second at slightly above double that, and the third at double the second. This doubling of amplitude for a perceptible change held true regardless of actuator placement or base amplitude.

Using the minimum perceivable amplitude as the lowest vibration intensity, the maximum number of non zero vibration intensity levels for the first armband would be 2. For the second armband, the maximum number of non zero vibration intensity levels would be 3, showing improvement.

9.3 FSR response

The following section discusses the results presented in section 8.2. For all measurement cases, the expected non linear inverse relationship between resistance and force was observed. While such a curve and relationship is described as a typical response in the data sheet, no exact relationship or equation is given. The data sheet also notes that the exact form of the curve will be determined by the surrounding mechanics, as was observed.

When the FSR is uncovered and the force exerted on it is on a small area, the force required to lower the resistance noticeably, i.e the break force, is comparable to that which is detectable by human skin. However, when the force is spread out to cover the whole active area of the sensor, and thereby decreasing the pressure, the force required increases significantly. This was notably observed when the sensor had no material covering it. Still, when covered by the dish-washing glove as well as when covered by the artificial skin material, the break force of the sensor was still low enough as to allow for a quite sensitive configuration.

The increase in breaking force when going between the totally uncovered sensor to the sensor and block configuration was expected. However, the decrease observed by adding a second interface material was not. No clear explanation for this has been found.

9.4 Power Consumption

The following section discusses the results presented in section 8.4. At full power, the actuators and their driving circuits are the most power hungry components of the system, followed by the encoders with accompanying low pass filters. During idle operation, when no contact is detected, the encoder circuit can be turned off using the transistor in figure 6.5. This was not done in the final version of the software as other issues could not be resolved in time.

With the discrete event feedback as the strategy, adding the energy usage of one vibration pulse for all the actuators, no significant extra power is drawn. However, the idle power draw of the system would amount to a significant portion of the total battery capacity. This difference could be partially offset by the possible reduction in gripping strength employed by prosthesis users, but no experiment was done to evaluate this.

9.5 Grip Testing

The following section discusses the results presented in section 8.12. The FSR sensitivity test showing that even when covered by artificial skin, the sensor would have a low break force. Despite this, only a few of the grip tests were successful, and only for rigid objects.

For both the pen and the water bottle, the position where the object made contact with the fingers had a profound impact on the ability of the sensor to detect touch. This indicates that even after adding the second FSR to create a parallel coupling to increase the active surface of the sensor, the parts of the fingers that were not covered by the sensors was still to large. This was especially apparent when the grip closed such that either only the very tip s or sides of the finger were in contact with the gripped object.

During the FSR test, the artificial skin was easily placed such that it rested flat against the sensor, leaving negligible air between the two. For the fingers, especially on the index finger, a gap between the skin and sensor was present. Due to the elastic nature of the artificial skin, this added an additional dead-band as the artificial skin would have to be compressed using a certain force before making contact with the sensor. This compression came in addition to the compression already needed to compress both the sensor and the skin when flat and tight.

9.6 Deformation Testing

The following section discusses the results presented in section 8.13. Due to the problems already observed during the grip testing, for all cases where deformation was applicable, contact detection failed, and thus no deformation could be detected. This failing of the system was due to no reliable contact detection being made, and thus the chosen algorithm failed. The proof of concept results indicate that better contact detection likely is the key to rectify the failure of the system.

9.7 Hardware

The following sections discuss the tests done on the hardware and the hardware implementation and integration with the Hy5 hand.

9.7.1 Force Sensors

The FSR was shown to have good performance when completely flat and with a cover that was fitted closely to perfectly, however the configuration and integration with the Hy5 hand used was non satisfactory. Both the sensitivity and the active area of the sensor were found to be lacking. Both the sensitivity and the active area of the sensors were found to be points where improvements could be made. To address the sensitivity issue, FSRs with a different range could be chosen, or a different type of sensor altogether. In addition, more care would have to be taken when covering the sensor. Having a springy material which diffuses contact forces and is pushed onto non sensitive parts of the finger was assesed to be a major problem, especially at first contact. If in the future FSRs are to be used in a commercial setting for the Hy5 hand, custom sensors could be ordered so that the active are of the sensor could be made to fit the finger perfectly.

9.7.2 Angle Sensors

The magnetic encoders and magnets allowed for integration with the hand without having to change parts of the Hy5 hand. The mounting of the encoders, especially for the proximal digits, was not structurally sound and failed on multiple occasions during testing. By mounting the encoders externally to the hand also meant that objects griped by the hand could come in contact with and possibly damage the sensors. For prototyping and testing out algorithms, having the encoders mounted externally on the prosthesis was acceptable, but for further development, internal angle measurement and cabling is recommended. Another issue with the external encoders was the magnets and their fields. These could potentially be a source of annoyance for users of the prosthesis.

The encoders were able to deliver a resolution of 1 degree. However, due to the logic level mistake made when ordering, see section 6.2.6, the filtered PWM signal was used by the ADC on the MCU. Due to the noisy nature of the signal no benefit could be seen using a 12-bit ADC resolution rather than the faster 8-bit. This would however give a slightly worse resolution at around 1.4 degrees.

9.7.3 Motor Drivers

The motor drivers proved suitable for the implemented architecture. Their low power consumption when not driving the actuators and size makes for easy integration within either a future armband or prosthesis socket.

The motor drivers were driven controlling the value of the amplitude register directly. If the same type of driver is to be used in the future, exploring the existing haptic library present on the ROM of the drivers is recommended.

For future use of similar motor drivers, chips with either controllable or different I2C addresses written in hardware, are preferred. While the solution found to the problem worked, it added unnecessary complexity and some small additional monetary cost.

9.7.4 Actuators and Armbands

The chosen actuators were easy to integrate within a small and simple armband. For the chosen LRAs only the amplitude of the vibration caused by the actuators was easily controllable. However, as shown in section 8.1 several intensity levels were possible to discern. Power consumption was relatively high when all actuators ran at maximum intensity, but when used in bursts as a part of a hand closing cycle, as presented in section 8.4, the added power draw was negligible.

The changes made when going from the first to the second armband aided in the easy of donning using one hand, and the ease with which one could ensure a tighter fit. For users of prostheses, easy donning is an important requirement.

The second armband also reduced the lowest perceivable stimulation intensity and increased the amount of discrete levels possible. This suggests that the combination of higher normal pressure and better contact between the actuator and skin through a rigid housing is important for haptic rendering.

9.7.5 MCU and Evaluation Board

The ATXmegaA3BU chosen, as well as the board used for evaluation proved more than powerful enough for the application made. Memory usage stayed below 20% for booth the data memory as well as the programming memory.

The IO of the MCU was also more than sufficient for the application. Even when each of the encoder inputs was analogue, there was enough ADC channels for the seven total analogue inputs. The two I2C busses avaliable would also allow for more actuators and drivers, provided that the I2C-address clashes would be resolved to avoid using more GPIO pins to control the state of the bus.

9.8 Software

The software was implemented as a ”big while loop” where each action runs to completion. To conserve power, between periodical wake ups, the system would enter a sleep mode. For the system as implemented with force sensing, angle sensing, deformation detection and actuator control, running as a while loop was sufficient.

9.9 Cost

The cost presented in section 8.3 shows that the components of the system costs less that 1000 NOK. While some additional cost is required, such as assembly, creating a custom PCB solution, passive components, and possibly creating a completely different solution for the armband, this is still a use-full estimate of the costs involved.

9.10 Acceptance Requirements

In this section the fulfilment of the acceptance requirements proposed in section 4.4 will be assessed.

1. Force Sensing
    (a) Be able to detect contact and release events. [Failure]
    (b) Differentiate between 2-4 force levels. [Success]
2. Vibration
    (a) Create discrete pulses of stimuli. [Success]
    (b) Create stimuli at different intensities. [Success]

3. Power Consumption

   (a) Reduce the total power used when gripping an object. [Not assessed]

   (b) Have power to run for at least 12 hours a day. [Not assessed]

4. Deformation Detection

   (a) Determine digit angles. [Success]

   (b) Combine the digit angles and force readings to determine if deformation is occurring. [Partial Success]

   The main point of failure is the failure of the force sensors system to reliably sense contact, particularly when holding or touching objects softly or touching objects that are fragile. This leads to only a partial success in deformation detection.

CHAPTER

TEN

CONCLUSION AND FUTURE WORK

10.1 Conclusion

Haptic feedback continues to be a requested feature in upper limb prosthesis, as explored in this thesis. The implemented architecture, with its hardware and software, created and tested as a part of this thesis shows some promise, however, more work is required for the system as it currently exists to be of much use. A main source of issues was the FSR sensors and their integration with the fingers. The sensor problems impacted all functional parts of the system, leading to a failure to reliably detect contact or deformation for non rigid objects. However, the force sensors were able to detect contact when grasping rigid objects, and were shown to be more sensitive given customisation and more careful integration better suited to the Hy5 hand.

10.2 Future Work

To better the functionality of the haptic feedback system, improvements to the force sensing system is required. If angle sensors are to be used in future iterations of the Hy5 hand, investigations into where and how to integrate such sensors into the finger digits is

required. Once a better sensory situation is achieved, miniaturisation and testing in more realistic settings using EMG control should be undertaken.

BIBLIOGRAPHY

Andresen, J. E. L., Dec. 2018. Haptic Feedback for Hydraulic Hand Prosthesis. Specialization Project at NTNU.

Antfolk, C., Björkman, A., Frank, S., Sebelius, F., Lundborg, G., Rosen, B., 2012. Sensory feedback from a prosthetic hand based on airmediated pressure from the hand to the forearm skin. Journal of Rehabilitation Medicine 44, 702–707.

Antfolk, C., D'Alonzo, M., Controzzi, M., Lundborg, G., Rosén, B., Sebelius, F., Cipriani, C., 2013a. Artificial redirection of sensation from prosthetic fingers to the phantom hand map on transradial amputees: Vibrotactile versus mechanotactile sensory feedback. IEEE Transactions on Neural Systems and Rehabilitation Engineering 21.

Antfolk, C., D'Alonzo, M., Rosén, B., Lundborg, G., Sebelius, F., Cipriani, C., 2013b. Sensory feedback in upper limb prosthetics. Expert Review of Medical Devices 10, 45–54.

Barone, D., D'Alonzo, M., Clemente, F., C, C., 2017. A cosmetic prosthetic digit with bioinspired embedded touch feedback. ICORR, 1136–1141.

Chapell, P., 2011. Making sense of artificial hands. Journal of Medical Engieering and Technology 35, 1–18.

Choi, S., Kuchenbecker, K., 2013. Vibrotactiledisplay:perception, technology, and applications. Proceedings of the IEEE.

Clemente, F., D'Alonzo, M., Controzzi, M., Edin, B., Cipriani, C., 2016. Non-invasive, temporally discrete feedback of object contact and release improves grasp control of

closed-loop myoelectric transradial prostheses. IEEE TRANSACTIONS ON NEURAL SYSTEMS AND REHABILITATION ENGINEERING.

Cordella, F., Ciancio, A., Sacchetti, R., Davalli, A., Cutti, A., Guglielmelli, E., Zollo, L., 2016. Literature review on needs of upper limb prosthesis users. Frontiers in Neuroscience.

Dahiya, R., Metta, G., Valle, M., Sandini, G., 2010. Tactile Sensing - From Humans to Humanoids. IEEE Transactions on Robotics.

Dietrich, C., Walsh, K., Preibler, S., Hofmann, G., Witte, O., Miltner, W., Weiss, T., 2012. Sensory feedback prosthesis reduces phanom limb pain, proof of a principle. Neuroscience Letters.

Electronics, I., 2019. FSR Integration Guide - Interlink Electronics. Interlink Electronics.

Fani, S., Di Blasio, K., Bianchi, M., Catalano, M., Grioli, G., Bicchi, A., 2019. Relayaing the high frequency contents of tactile feedback to robotic prosthesis users: Design, filtering, implementation and validation. IEEE Robotics and Automation Letters.

Gentilucci, M., Toni, I., Daprati, E., Gangitano, M., 1997. Tactile input of the hand and the control of reaching to grasp movements. Experimental Brain Research 114, 130–137.

Hy5, 2017. Hy5 service manual.
URL `https://www.hy5.no/our-products`

Johannson, R., Edin, B., 1993. Predictive feed-forward sensory control during grasping and manipulation in man. Biomedical Research 14, 95–106.

Johansson, R., Flanagan, J., 2009. Coding and use of tactile signals from the fingertips in object manipulation tasks. Nature Reviews 10, 345–359.

Kaczmarek, K., Webster, J., Bach-y Rita, P., Tompkins, W., 1991. Electrotactile and Vibrotactile Displays for Sensory Substitution System. IEEE Transactions on Biomedical Engineering.

Kawato, M., 1999. Internal models for motor control and trajectory planning. Current Opinion in Neurobiology.

Mahns, D., Perkins, N., Robinson, S., Rowe, M., 2005. Vibrotactile frequency discrimination in human hairy skin. Journal of Neurophysiology.

Marasco, P., Kim, K., Colgate, J., Peshkin, M., Kuiken, T., 2011. Robotic touch shifts perception of embodiment to a prosthesis in targeted reinnervation amputees. Brain.

Merzenich, M., Harrington, T., 1969. The sense of flutter-vibration evoked by stimulation of the hairy skin of primates: Comparison of human sensory capacity with the responses of mechanoreceptive afferents innervating the hairy skin of monkeys. Expreimental Brain Research.

Motamedi, M., Otis, M., Duchaine, V., 2017. The Impact of Simultaneously Applying Normal Stress and Vibrotactile Stimulation for Feedback of Exteroceptive Information. Journal of Biomechanical Engineering 139.

Raveh, E., Portnoy, S., Friedman, J., 2018. Adding vibrotactile feedback to a myoelectric-controlled handimproves performance when online visual feedback is disturbed. Human Movement Science.

Schoepp, K., Dawson, M., Schofield, J., Carey, J., Herbert, J., 2018. Design and integration of an inexpensive wearable mechanotactile feedback system for myoelectric prostheses. IEEE Journal of Transtaional Engieering in Health and Medicine 6.

Yamada, H., Yamanoi, Y., Wakita, K., Kato, R., 2016. Investigation of cognitive strain on hand grasping induced by sensory feedback for myoelectric hand. In: IEEE International Conference on Robotics and Automation. IEEE International Conference on Robotics and Automation, pp. 3549–3554.

Appendix A
Code

This appendix describes the functions written for this project and where to find them. The sections correspond to the modules in diagram 6.6. The code is found in the accompanying files.

main

All functions part of the main module are found in main.c

```
// Timer Counter ISR toggling and LED every second
static void timer_light_isr(void);

// Timer Counter ISR triggering a FSR reading every ms
static void timer_fsr_isr(void);

// Timer Counter ISR triggering a encoder reading every 0.1 second when
    contact is detected.
static void void timer_enc_isr(void);

// Timer Counter ISR responsible for controlling vibration pulsing.
    Triggered every 0.1 second.
static void timer_pulse_counter_isr(void);

// Initialises the timers used by the main function
static void timer_init(void);

// Initialises the MCU, board and modules used by the main board directly
static void system_init(void);

// Primary application. Called after system initialisation and optional
    calibration is complete.
static void haptic_feedback_state_machine_speed_based(void);

// Main function. Calls initialisation functions for all modules and
    starts the state machine.
int main(void);
```

force_sensors

All function implementation is found in the file force_sensors.c.

Public Functions Declared in the File force_sensors.h

```
// Initialises the ADC used by the FSRs and configures the IO ports used. Calls the calibration routine if calibrate = 1.
void force_sensors_init(uint8_t calibrate);

// Reads the raw values from the ADC and places them in the array pointed to by *results.
void force_sensors_read(uint16_t *results);

// Reads the raw values from the ADC, converts them to discrete levels defined by the initialisation function. Places the results in the array pointed to by *force_levels.
void force_sensors_read_force_levels(uint8_t *force_levels);

// Reads force levels, but with a Schmitt trigger like hysteresis to reduce the jumping between levels around the level boarders.
void force_sensors_read_force_levels_with_hysteresis(uint8_t *force_levels);
```

Private Functions Declared in the File force_sensor.c

```
// Saves calibrated values to the EEPROM. Sets the byte in the EEPROM which indicates data is saved.
static void force_sensors_save_to_eeprom(void);

// Reads previous calibration data from the EEPROM and saves it to the correct variables.
static void force_sensors_read_from_eeprom(void);

// Based on either calibration data or default values, the force level boarders are created using a function to counter the non linearity of the FSR.
static void force_sensors_create_levels(void);

// Performs the calibration if calibrate = 1. Else, uses stored data or default values when calling force_sensors_create_levels()
static void force_sensors_calibrate(uint8_t calibrate);
```

vibration_actuators

All function implementation is found in the file vibration_actuators.c.

Public functions declared in the file vibration_actuators.h

```
1 // Initialised the I2C module (called TWI), sets up the IO pins for I2C
      and the driver selection. Finally runs the autocalibration routine.
2 status_code_t vibration_actuator_init(void);
3
4 // Selects an actuator and set one of the predefined amplitudes.
5 void vibration_actuator_set_amplitude_level(uint8_t actuator_no ,uint8_t
      level);
6
7 // Sets the amplitude of all actuators to 0.
8 void vibration_actuator_all_off(void);
```

Private functions declared in the file vibration_actuators.c

```
1 // For the actuator currently selected, set the amplitude without using
      the predefined levels.
2 static void vibration_actuator_set_amplitude(uint8_t amplitude);
3
4 // Selects an actuator by setting the pin corresponding to the selected
      actuator to a high impedance mode. The remaining actuators are set as
      output and pulled high. This ensures only one motor driver receives
      the I2C start condition.
5 static status_code_t vibration_actuator_select_actuator(uint8_t
      actuator_no);
6
7 // Sets up and runs the auto calibration as described in the data sheet
      for the motor driver.
8 static void vibration_actuator_autocalibrate(uint8_t actuator_no);
```

magnetic_encoders

All function implementation is found in the file magnetic_encoders.c.

Public Functions Declared in magnetic_encoders.h

```
// Initialises the ADC used for angle reading and sets up ADC pins and the
    pin used to control the power to the encoders.
void magnetic_encoders_init(void);

//Pulls the pin controlling the power to en encoders high.
void magnetic_encoders_enable(void);

//Pulls the pin controlling the power to en encoders low.
void magnetic_encoders_disable(void);

// Reads the encoder values and translates the results into angles.
void magnetic_encoders_read_angle(int16_t angles[NO_OF_ENCODERS]);
```

Private Functions Declared in magnetic_encoders.c

```
// Loads default values for use when translating between ADC values and
    angles. Was meant to be a part of a future calibration routine.
static void magnetic_encoders_load_min_max_values(void);

// Starts the ADC conversion and returns the results to the array pointed
    to by results[NO_OF_ENCODERS]
static void magnetic_encoders_read_raw(int16_t results[NO_OF_ENCODERS]);
```

buttons

All function implementation is found in the file buttons.c

Public Functions Declared in buttons.h

```
1 // Initialises the timer used by the button module
2 void buttons_init(void);
```

Private Functions Declared in buttons.c

```
1 // Timer Counter ISR polling the state of the buttons on the evaluation
      board. If a state change from not pressed to pressed is detected, the
      variables button_switched[X] is set and can be read and cleared by
      modules using the button module.
2 static void timer_buttons_isr(void);
```

test_functions

All functions are found as comment blocks in test_functions.c. Most of these functions were used to conduct the tests described in chapter 7.

```
1  //Haptic feedback state machine based around total angle changes since
       contact rather than angle speed
2  static void haptic_feedback_state_machine_change_based(void);
3
4  // Function for testing how low of an amplitude user can feel for each
       actuator.
5  static void min_amplitude_detectable(void);
6
7  // Function for testing how small of an amplitude difference a user can
       feel for each actuator.
8  static void min_amplitude_difference(void);
9
10 // Using the list at the beginning, pulse the an actutor and wait for a
       button press to pulse the next
11 static void test_which_vibrator_pulsing(void);
12
13 // Using the list at the beginning, pulse the two actuators and wait for a
        button press to pulse the next pair.
14 static void test_dual_vibrator_pulsing(void);
15
16 // Selects the two actuators which are not actuator_not_active, sets their
        amplitude to level, delays for duration, then calls
       vibration_actuators_all_off().
17 static void vibration_actuator_dual_pulse(uint8_t duration, uint8_t level,
        uint8_t actuator_not_active);
18
19 // Selects an actuator, sets the amplitude level, sleeps for duration then
        set the amplitude to 0.
20 static void vibration_actuator_pulse(uint8_t actuator_no, uint8_t level,
       uint8_t duration);
```

Appendix B
Pictures of Hardware

This appendix shows the hardware as it was at time of thesis delivery.

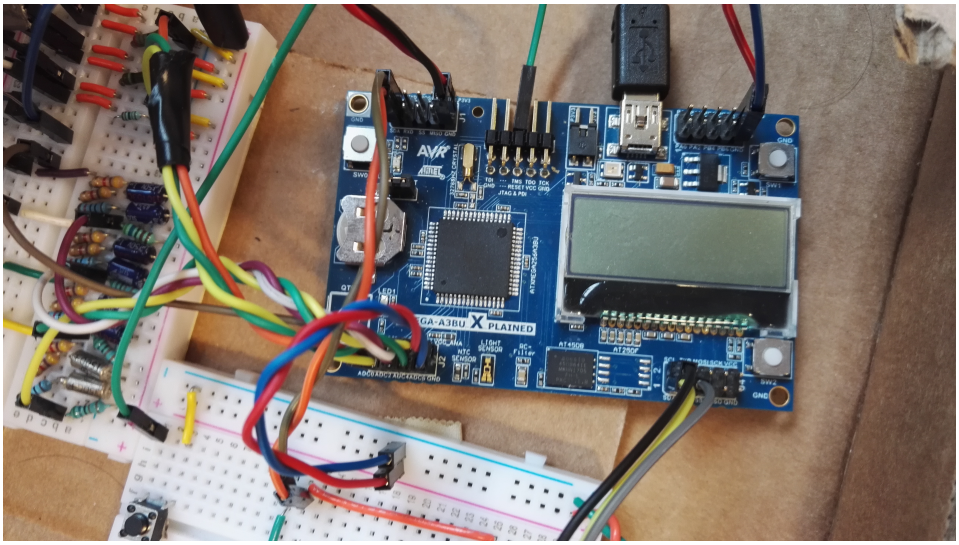

Figure 10.1: Picture of the evaluation board.

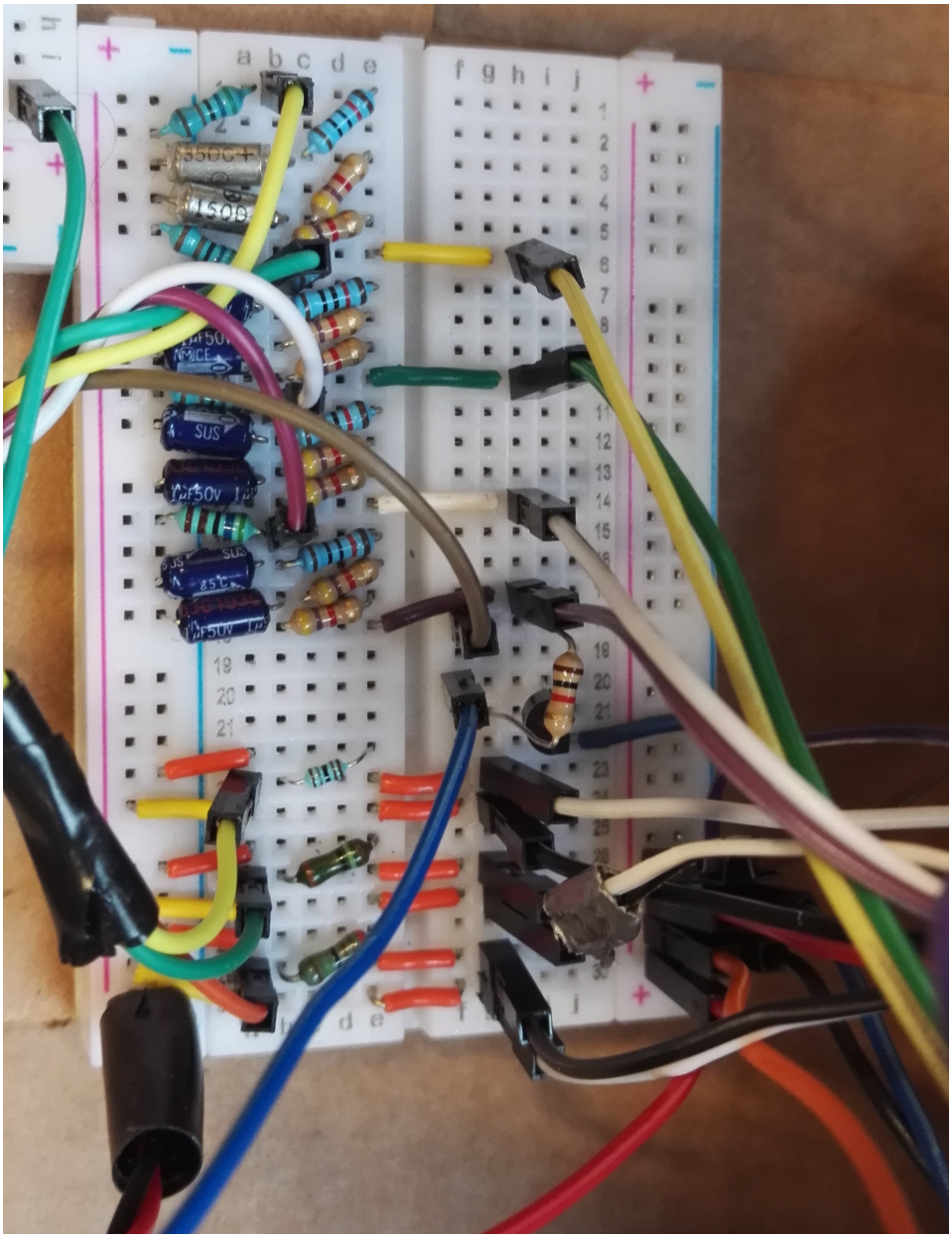

Figure 10.2: Picture of the low pass filters, in the top left, shown schematically in figure 6.5. In the lower left, the voltage dividers for the FSRs, as shown schematically in figure 6.4, are placed.

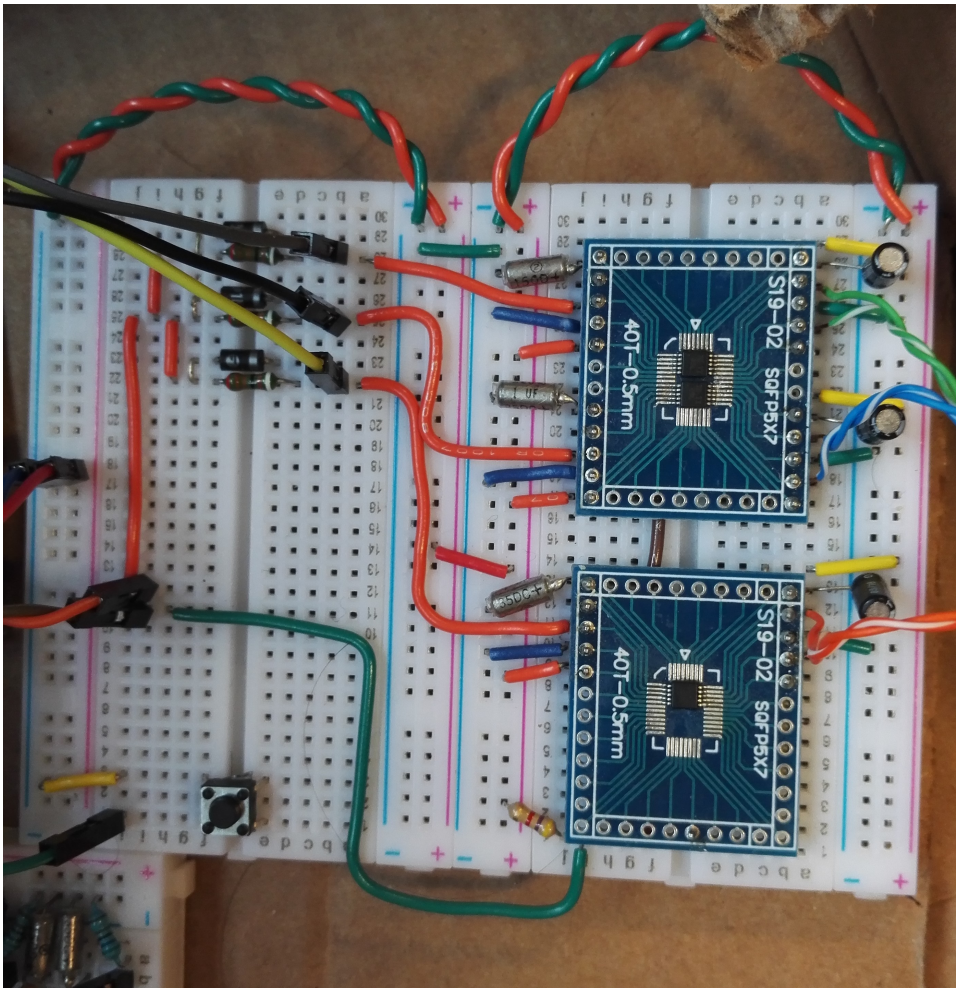

Figure 10.3: Picture of the motor drivers, I2C control and reset button. The motor drivers are shown schematically in figure 6.2. The orange, blue and green cables to the very right connect to the actuators in the armband.

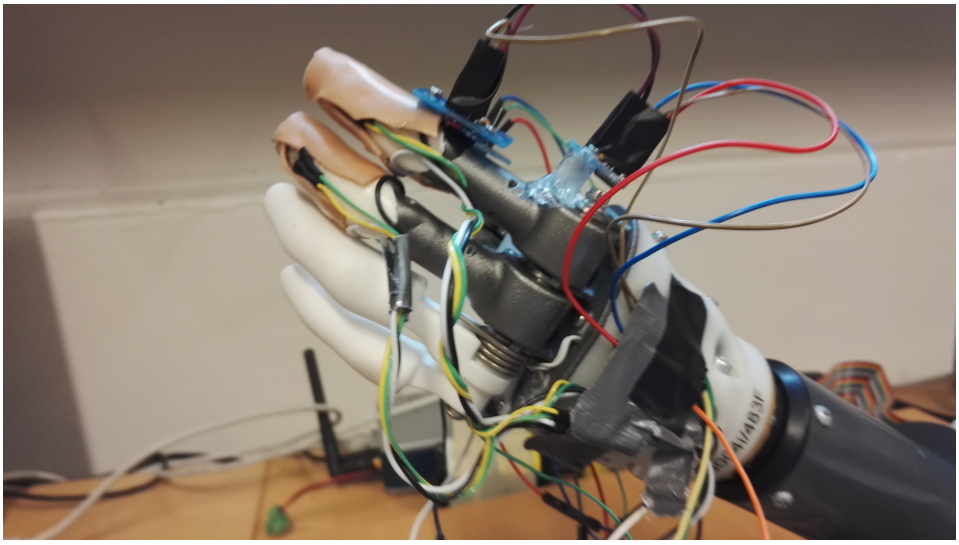

Figure 10.4: Picture of the Hy5 hand with all sensors mounted. The black, white, green and yellow cables coming from the middle and index fingers are connected to the force sensors. The other cables are for the encoders.

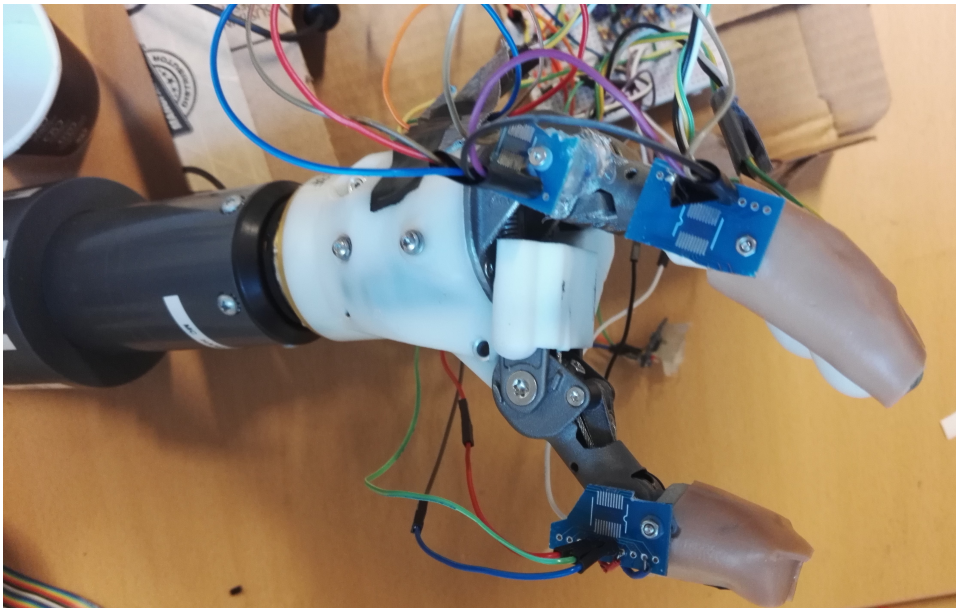

Figure 10.5: Picture of the Hy5 hand with all sensors mounted. The thumbs proximal encoder would be placed on the opposite side of the distal, had it not fallen off before this photo was taken.

Figure 10.6: Picture of the first armband.

Figure 10.7: Picture of the second armband.

Figure 10.8: Picture of the first armband, worn on the upper arm.

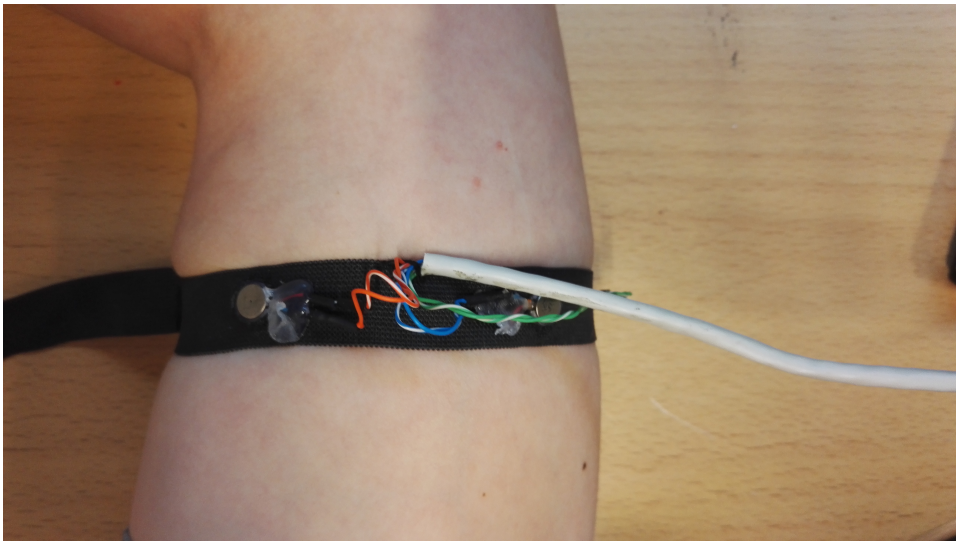

Figure 10.9: Picture of the second armband, worn on the upper arm.

Figure 10.10: Picture of the second armband, worn on the upper arm.

Appendix C
Overview of Attached Files

The zip accompanying this report contains to following:

- 3D-files Used for Printing
  - Housing for LRA.stl
  - Stand off for Index finger.stl
  - Stand off for Thumb.stl
- Code
  - HapticFeedback1.atsln (Atmel Studio Project)
  - HapticFeedback1, folder containing all source code. Code produced during this project is found under src.
- Video Grip and Deformation
  - Video files which formed the basis of the tests described in 7.5 and 7.6.
- Haptic Feedback for Hydraulic Hand Prosthesis 2018.pdf

Appendix D
Specialisation Project

This master thesis is a continuation of the work and study completed during the fall of 2018. The associated reports for both the thesis and the specialisation project are both not to be published until some time has passed. Therefore, the report from the specialisation project, Andresen (2018), is appended in its entirety.

TTK4550 - Engineering Cybernetics, Specialization Project

Haptic Feedback for Hydraulic Hand Prosthesis

Jon Eirik Lisle Andresen
December 18, 2018

Supervisors:
Øyvind Stavdahl
Bjørn Olav Bakka

Department of Engineering Cybernetics
Norwegian University of Science and Technology

Summary

This report is a study of haptic feedback for upper limb prostheses, and in particular related to the Norwegian company Hy5's hand. The report starts with a theory section about haptic feedback, sensors and actuators, human sensory systems in the skin and motor control. Then, the relevant aspects of the Hy5 hand are presented.

Three different architectures are then presented and discussed, before reaching a conclusion that a system based on sensors in the fingers of the prosthesis and actuators on the skin of the user is most suited. This architecture is chosen due to its versitility and adaptability. Future work includes building a prototype and validating if such a system could further increase the benefits of using the Hy5 hand.

Sammendrag

Denne rapporten er et studie av haptisk tilbakekobling for håndproteser, med spesielt fokus på det norske firmaet; Hy5, sin hånd. Rapporten begynner med en teoridel om haptisk tilbakekobling, sensorer og aktuatorer, sensoriske systemer i huden og menneskelig styring av bevegelse. Deretter blir de relevante delene av Hy5 hånden presentert.

Tre forskjellige arkitekturer blir så presentert og diskutert, før en konklusjon om at et system basert på sensorer i protesens fingre og aktuatorer på brukerens hud er best egnet. Denne arkitekturen ble valgt da den er enkel å tilpasse. Fremtidig arbeid arbeid inkluderer å bygge en prototyp og validere at et slikt system kan øke fordelene ved å bruke Hy5's hånd.

Problem Description

The Norwegian firm Hy5 AS develops hand prosthesis for people lacking a hand and/or part of an arm, either due to a congenital disorder or a traumatic amputation. To give the user the best possible conditions for controlling the motion of the prosthesis in an accurate manner, implementing a form of haptic feedback is desirable. Meaning that information about forces, velocities, and/or joint angles in the prosthesis are conveyed to the user through one or more ways of stimulation (mechanically or electrically), and thus in principle some of the mechano sensory abilities lost due to amputation is restored. Through this project, you shall explore and possibly test suitable sensor and actuator modalities as well as complete algorithms for the haptic feedback system.

- Provide an overview of terms and techniques within the field of haptic feedback in robotics and tele-manipulation in general, but with an added emphasis on earlier research related to upper limb prosthesis. The overview should cover the physiological structures (mechano receptors in the skin etc.) the equipment will interact with, and sensor and actuator modalities, and different algorithms and philosophies attempted in the past.
- Assess how compatible the findings from part 1 are in regards to the existing prosthetic system.
- Make a justified choice of architecture, algorithms and actuator and sensor technology for haptic feedback for the Hy5 prosthesis, and make an assessment of which aspects of the resulting system are most uncertain.
- To the degree which time allows, make a physical setup, demonstrating and evaluating the planned system. Priority should be given to the uncertain components of part 3 whenever a decision has to be made regarding what to implement and test.

TABLE OF CONTENTS

Summary i

Sammendrag i

Problem Description ii

Table of Contents iv

Abbreviations v

1 Introduction 1
- 1.1 Powered Upper Limb Prostheses . . . 1
- 1.2 Haptic Feedback . . . 1
- 1.3 Motivation . . . 2

2 Theory 3
- 2.1 Human Sensor Array . . . 3
  - 2.1.1 Mechano Receptors . . . 3
  - 2.1.2 Proprioception . . . 4
- 2.2 Motor Control in Humans . . . 4
- 2.3 Sensors . . . 5
  - 2.3.1 Force Sensors . . . 5
- 2.4 Actuators . . . 6
  - 2.4.1 Stimulation by Sensory Substitution . . . 6
  - 2.4.2 Modality Matched Stimulation . . . 7
- 2.5 Targeted Muscle and Sensory Re-innervation . . . 7
- 2.6 Phantom Limb Maps . . . 8

3 Hy5 Hand 9
- 3.1 Hydraulic system . . . 10
- 3.2 Adaptive grip . . . 10
- 3.3 Current Control System . . . 10

4 Method and Previous Work **11**
4.1 Literature Review . . . 11
4.2 Previous Work . . . 11
4.2.1 Schoepp, K. *et. al.* . . . 12
4.2.2 Antfolk, C *et. al.* . . . 12
4.2.3 Aboseria, M. *et. al.* . . . 12
4.2.4 Barone, D. *el. al.* . . . 13

5 Proposed Architectures **15**
5.1 Sensors on Hand . . . 15
5.2 Hydraulic or Pneumatic System . . . 15
5.3 Using EMG-signal . . . 16

6 Discussion and Results **17**
6.1 Discussion of Previous Work . . . 17
6.1.1 Schoepp, K. *et. al*, see 4.2.1 . . . 17
6.1.2 Antfolk, C *et. al*, see 4.2.2 . . . 17
6.1.3 Barone, D. *et. al*, see 4.2.3 . . . 17
6.2 Discussion of Proposed Architectures . . . 18
6.2.1 Sensors on Hand. See 5.1 . . . 18
6.2.2 Hydraulic or Pneumatic system. See 5.2 . . . 18
6.2.3 Using EMG-signal. See 5.3 . . . 19
6.3 Choosing MCU-based system . . . 19

7 Conclusion and Future Work **21**
7.1 Conclusion . . . 21
7.2 Future Work . . . 21

Bibliography **21**

Abbreviations

EMG	=	Electromyography
CNS	=	Central Nervous System
PNS	=	Peripheral Nervous System
FA	=	Fast Adapting
SA	=	Slow Adapting
TMSR	=	Targeted Muscle and Sensory Re-innervation
MCU	=	Micro Controller Unit
FSR	=	Force Sensitive Resistor

CHAPTER

ONE

INTRODUCTION

1.1 Powered Upper Limb Prostheses

Prosthetic replacements of missing limbs, either due to amputation or a condition existing at birth, is an old medical technique. An early powered design can be found as 1915 Germany [10], where the prosthetic hand was powered by pneumatics. During the 1960s, using surface electromyography (EMG) on residual limbs became available for commercial prostheses, and is currently the most used source of a control signal in powered upper limb prostheses [20]. The EMG signal is produced by a contracting muscle or muscle group, and is detected by a set of electrodes placed on the users skin. While this gives the user a clear, if not direct, link from intent to prosthesis movement there is little flow of information the other way, other than incidental clues like motor noise and vibration.

1.2 Haptic Feedback

When providing haptic feedback to the prosthesis user, one can either attempt to stimulate with the same modality as is measured, or through some substitute channel. When the measured entity matches the modality used as feedback we say we use modality matched feedback. An example is a force sensor placed on the fingertip of a prosthesis digit which causes a linear tactor to impart a force in the users skin. Whenever the feedback is on a form that is different what is sensed, it is said that the feedback takes the form of sensory substitution, such as force levels represented as a vibration. Most research into the field of sensory feedback for upper limb prosthesis uses sensory substitution [3].

In addition to modality, the somatotopic matching, the perceived location of the stimuli, is important for the quality of the feedback to the user [15]. Most simple and early research into haptic feedback lacks somatotopic matching.

1.3 Motivation

Not having a hand reduces functionality. Not only the ability to manipulate physical objects, but also the ability to gather information about them is lost. Currently there are no commercially available powered upper limp prosthesis who supply the user with tactile or haptic feedback other than forces transferred through the prosthesis itself. Regaining some of the sense of touch can increase embodiment [18], reduce phantom pain [9] and increase the ability to use the prosthesis without using visual feedback [25]. All of these points combined can explain why users often cite haptic feedback, or lack thereof, as a reason for prosthesis abandonment [8].

CHAPTER

TWO

THEORY

2.1 Human Sensor Array

When a loss of limb occurs, several sensory functions are lost. For a healthy human, information about touch, proprioception, pain and temperature is transmitted from nerve endings in the skin, muscles and tendons of the hand and arm, through the peripheral nervous system (PNS), to the central nervous system (CNS), where the signal is interpreted and used.

2.1.1 Mechano Receptors

The glabrous skin found in the human hand contains several different types of nerve cells responsible for mechanical sensations, such as force, vibration and texture, temperature and pain. The focus of this paper will be the mechanical sensations, as they are the most closely related to the control input of the prosthesis and therefore the most useful when forming a closed loop control circuit.

There are four different classes of mechanoreceptors responsible for the mechanical sensations in humans. These differ in function, receptive fields and adaption rates. The different cells can be divided by their adaption rate, into fast adapting (FA) type I and II, and slow adapting (SA) type I and II. A summary of the different functions can be found in table 2.1, based on [16].

	Fast Adapting (FA)	
	Meissner corpuscles (FA I)	*Pacinian corpuscles (FA II)*
Receptive field	Small, sharp	Large, diffuse
Density $\left[\frac{\text{units}}{\text{cm}^2}\right]$	140	20
Spatial Resolution [mm]	3-4	10
Stimulation Frequency [Hz]	5-50	40-500
Sensory Function	Vibration detection. Temporal change in skin deformation.	High frequency vibration detection. Temporal change in skin formation.
	Slow Adapting (SA)	
	Merkel cells (SA I)	*Ruffini endings (SA II)*
Receptive field	Small, sharp	Large, diffuse
Density $\left[\frac{\text{units}}{\text{cm}^2}\right]$	70	10
Spatial Resolution [mm]	0.5	7
Stimulation Frequency [Hz]	0.4-40	<7
Sensory Function	Static force detection. Form detection. Texture perception.	Static force detection. Finger position determination Tangential force detection

Table 2.1: Overview of mechanoreceptors found in glabrous human skin. Adapted from [16]

The receptive field of a mechanoreceptor is the area of the skin where a nerve ending can detect stimuli, the density is the amount of cells pr unit of area, the spatial resolution is the smallest distance between two stimuli that will result in a ”double” sensation, the stimulation frequency is the frequency range detectable by the receptor.

2.1.2 Proprioception

Proprioception is the sense of the relative position of joints and limbs of the body [24]. Information about muscle extension, tension in tendons and joint position is transferred from nerves within muscle, tendons, joints and skin to the CNS. In addition to the use by the CNS, proprioception is an integral part of human reflexes. This includes relaxing muscles when an overloading is detected and compensation for an abrupt increase in load [24].

2.2 Motor Control in Humans

During manipulative task, the time between an error episode and the corresponding corrective action is at least 45 ms, which will yield a maximum control signal frequency of 1 Hz, which is slower than many manipulation tasks [12], and thus motor control cannot only rely on continuous feedback control.

In [13], Johansson et.al. argues that the role of feedback in such a feed-forward system is to detect the transition of action phases; the different phases of manipulation task. The

transitions of such phases takes the form of discrete events detectable by the PNS and in turn the CNS.

Johansson also argues that the tactile information is used to update internal models such that the same object or similar objects can be manipulated according to an updated feed forward scheme in the future. The theorised internal models include both the expected tactile feedback from external objects, as well as the feed-forward commands necessary to complete a desired trajectory of motion [14].

2.3 Sensors

The four mechanoreceptors discussed previously all respond to external forces, either normal forces or tangential forces. Based on their adaption rates and frequency ranges, they exhibit a varied sensitivity to vibration as well as to sustained pressure. There are also sensory organs responsible for detection and monitoring of relative joint position. The following section will outline different classes of sensors that can be applied to fulfil the task of the lost neural sensors. For reviews of tactile sensing see [31], [17] and [3].

2.3.1 Force Sensors

When gripping an object, sufficient force must be applied such that the friction force between the hand and object can overcome the pull of gravity. However, with coefficients of static friction varying by several orders of magnitude, the force required to lift and hold an object varies not only with the mass of the object, but also with its surface properties. This in effect creates a lower bound for the force to be applied. Objects to be held will also be crushed at different force levels, putting an upper bound on the force to be applied.

Strain Gauges

A strain gauge is a resistor, or set of resistors which resistive values change with deformation. Strain gauges are long resistors adhered to a plastic or plastic like film. When strain is applied to the strain gauge, the resistance across its two terminals changes. Strain gauges exhibit a high sensitivity, but are susceptible to noise from temperature change and humidity. To combat temperature sensitivity, a Wheatstone configuration is often employed. Strain gauges can be made with high spacial resolution and high sensitivity and are a well established technology.

Force Sensitive Resistor (FSR)

An FSR is a material which resistance changes with applied force and consists of layers of polymer materials. FSR's have a non-linear response, in that they show a higher sensitivity at lower applied forces [7]. While the FSR has a high degree of sensitivity, the variability is also high. Hysteresis is also present in an FSR. The FSR is also sensitive to noise from temperature changes [7].

An FSR can be made with dimensions at least as thin as $200\mu\mathrm{m}$ as well as flexible enough to be fitted around a prosthetic finger, and can be manufactured at a low cost [25].

Capacitive Sensors

A capacitve sensor can be made by mounting two capacitive plates with an isolating or dielectric material in between [19]. A known relationship between deformation and force and between deformation and capacitance can be exploited to measure the applied force. Capacitive sensors are generally accurate, sensitive and can detect both static and dynamic forces. They also consume little power. This comes at the cost of higher prices and a need for more complex electronics. [16]. Capacitive sensors can be made vary thin and with a small cross-section.

Optical Sensors

An optical sensor consists of a light source, a transduction material and a light detector. When light from the source passes through the transduction material, the light is modulated in proportion to the force or pressure applied to the transduction material [22]. Optical sensors require extra circuitry and are generally large and fragile. At the same time optical sensors yield a high spatial resolution and is close to immune to electromagnetic fields.

Piezoelectric Sensors

Piezoelectric materials generate voltages when deformed by an external force. This generate voltage can be used in a piezoelectric sensor to sense changes in forces. Such sensors are reliable, fast and require no external power-supply. However, by their nature only dynamic forces can be detected, and at a low resolution [16].

2.4 Actuators

In the following sections, four ways of creating a sensation of mechanical stimulation will be discussed. Vibrotactile, creating a mechanical vibration [4], electrotactile, stimulating the skin and nerves with electric pulses, normal force [16], pushing the skin via some actuator creating a force normal to the skin [23], and direct nerve stimulation where a stimulator is implanted under the skin to directly stimulate a nerve ending to emulate signals coming from mechanoreceptors [29].

2.4.1 Stimulation by Sensory Substitution

Vibrotactile stimulation

In vibrotactile stimulation, information of some state is conveyed to the prosthesis user via some vibrating actuator. By its vibrational nature, several physical aspects of the wave can be used to transmit information to the user. This includes frequency, amplitude and different wave-forms, with frequency and amplitude the most common information carriers.

To stay withing the frequency range of the fast adapting type II mechano receptors, see table 2.1, staying within $50 - 300\text{Hz}$, as recommended in [16], will achieve this.

Electrotactile Stimulation

In electrotactile stimulation, information is conveyed to the prosthesis user via a small, low power electrode. The application of either a controlled current or voltage on an area of the skin stimulates nerves close to the stimulation site creating a sensation of mechanical stimuli for the user.

The sensation created by electrotactile stimulation is reported as ”a tingle, itch, vibration, touch pressure, pinch, and sharp and burning pain depending on the stimulating voltage, current and waveform, as well as on the electrode size, material and contact force, and the kin location, hydration and thickness” [3].

By the electric nature of electrotactile stimulation, the generated voltage and current can interfere with EMG-sensors placed in close proximity to the actuators. To mediate this, extra filtering of the EMG signal or time multiplexing, i.e switching between stimulation and EMG detection, can be included in the prosthetic system.

2.4.2 Modality Matched Stimulation

Normal Force Stimulation

In vibrotactile stimulation, information of some state is conveyed to the prosthesis user via a linear actuator pressing down on the skin. A normal force stimulator can take the form of a motor driving a shaft onto the skin, but the required pressure can also be created by hydraulics or pneumatics.

Direct Nerve Stimulation

In direct nerve stimulation, an electrode is implanted to directly electrically stimulate the remaining nerves in the residual limb. In contrast to the previously presented stimulation techniques, direct nerve stimulation is highly invasive as it requires much closer access to the subjects PNS. By implanting a small electrode by or around an afferent nerve ending it is possible to start the propagation of an action potential.

By stimulating parts of the PNS directly, a layer of abstraction and cognitive load is clearly removed from the user. However, currently the signal perceived by user is often reported as feeling unnatural and foreign. This is thought to be caused by the fact that direct nerve stimulation stimulates a large section of nerve fibres and without consideration being taken in regards to the relative timing of their firing [13].

A way of minimising the inherent risks involved with having electrode wires piercing the skin is to fasten the prosthesis to the body via osseointegration [6], integrating a metal bolt into the skeletal system. Using the metallic connector for the prosthesis as a sterile and structurally sound way into the body could aid the viability of direct nerve stimulation.

2.5 Targeted Muscle and Sensory Re-innervation

To address the issue of somatotopic matching, targeted muscular and sensory re-innervation (TMSR) surgery may prove useful. In TMSR, motor and sensory nerves are rerouted from the residual limb to other parts of the body [27]. Thus, by moving the nerve endings from

the residual limb to, for example the chest area, one can achieve somatotopic matching to a higher degree and also increase the possible areas of stimulation.

2.6 Phantom Limb Maps

As demonstrated in [11] by Ehrsson et. al. and exploited in [2] by Antfolk, many who have undergone an upper limb amputation experience that stimulation of specific areas of the residual limb cause a sensation of the missing limb being stimulated. The phenomenon is called a phantom limb map. A study, by Björkman et.al [5] showed that the same areas of the primary somatosensory cortex were activated when stimulating the phantom limb map as in a control group consisting of unimpaired individuals. For prosthesis users with a phantom limb map, either complete or partial, a higher degree of somatotopic matching can be achieved than without, and this is thought to increase ownership over the prosthesis and reduce the training time needed to effectively utilise the haptic feedback [2].

CHAPTER

THREE

HY5 HAND

Hy5 is a Norwegian company with offices in Raufoss and Oslo. At time of writing Hy5 offers a myoelectric prosthetic hand where the delivery of torque to the fingers is done via hydraulics. Through the use of 3d-printed and lightweight components, an adaptive grip where the digits of the fingers close in a natural fashion, and hydraulics, rather than an array of electric motors, Hy5 achieves a relatively high degree of functionality while maintaining robustness and keeping expenses down [28].

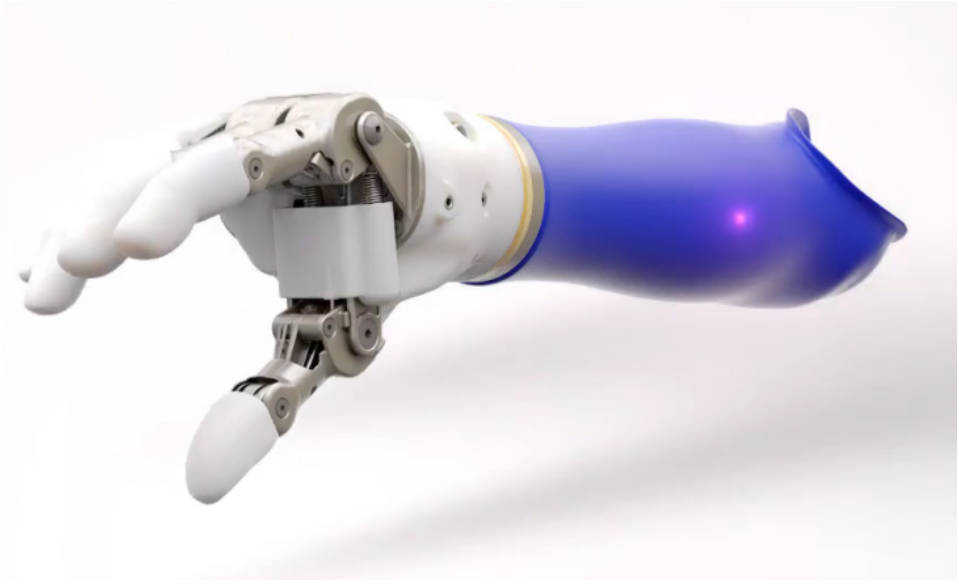

Figure 3.1: A computer generated illustration of the current Hy5 hand with a socket i blue attached.

3.1 Hydraulic system

The main difference between the Hy5 hand and other available prosthetic hands is the reliance on hydraulics. For a comprehensive look at the the design see the patent for the pump assembly [21]. The Hy5 hand employs a single electric motor driving a high pressure, low volume pump and a low pressure, high volume pump. By running the high volume pump until contact with an object and the subsequent build up of pressure, the hand can close with a high speed, but still achieve a high maximum gripping force due to the inclusion of two different pumps. Both pumps pumps fluid such that pressure builds up behind the middle finger, index finger and thump, however, when the hand has closed around an object, only the high pressure pump is in action.

3.2 Adaptive grip

The fingers are designed such that the force provided is balanced between the index and middle finger and the thumb. These three fingers have a secondary digit, distally, as an approximation of a normal human finger. When contact between a finger and an object occurs, the part of the finger, or the finger that made contact will stop its motion, while the pressure will be transferred to the other fingers, such that every finger will move until all are in contact. By a system of wires and springs, the top digit of a finger will keep moving should the bottom part reach an object.

This automatic and equal distribution of forces, combined with the finger digit design, allows the Hy5 hand to grasp a multitude of different shapes.

3.3 Current Control System

The Hy5 hand has one control input, which controls the speed of the motor. This, in turn, builds up pressure. The control input to the motor can be sourced from the difference between to antagonistic muscle groups, giving the user some control of the motor speed and thus of the pressure and torque produced.

The design of the fingers and their cable configuration, the hand is only able to provide significant force when closing. The opening of the fingers is provided by a configuration of springs in the fingers and by the opening of valves allowing hydraulic fluid to flow from the finger side of the hydraulic system.

CHAPTER

FOUR

METHOD AND PREVIOUS WORK

4.1 Literature Review

To gain an understanding of the subject at hand, a literature review was undertaken.

First, an understanding of the current state of myoelectric upper limb prosthesis was sought out. This is a mature field, with several commercial actors and a large literature bank, including books such as [20] by Muzumdar. The understanding gained consisted of understanding the origins of the myoelectric signal; the propagating action potential along a contracting motor unit. Then, when the source of the control signal was understood to a sufficient degree, an understanding of how the myoelectric signal can be used to control one or more states of a prosthesis was acquired.

After having gained a sufficient understanding of upper extremity prosthesis and the myoelectric signal in general, it was decided that the focus would be directed towards haptic feedback, and to relate that to the Hy5 hand. With the focus shifted to an aspect of prostheses without the same level of commercialisation, the source of information became research articles and papers. The first objective was to get an overview of the field.

To understand the role of feedback in prosthesis, an understanding of feedback in motor control for the unimpaired was sought. First, an overview of what is sensed by the receptors in a human hand was examined. Then, the role of said feedback in motor control was examined.

Then, in parallel , the literature study was focused on previous works on haptic feedback in upper limb prosthesis. To understand how to create something useful for the Hy5 hand, an understanding of different schools of thought and architectures was sought. Different sensors and actuators were looked into, both as parts of a whole system, and as individual components.

4.2 Previous Work

In this section, some of the previous works on haptic feedback is presented. Note that this represents only a small fraction of the studies and articles published.

4.2.1 Schoepp, K. *et. al.*

In [25], capacitive sensors are placed under a layer of nitrile on the thumb and index finger on an existing prosthesis. The forces detected by the sensors were then transferred, via a MCU embedded into the arm of the prosthesis, to specially designed tactors; small motors which pushed down on the skin, creating a linear force sensation on the skin of the prosthesis user. The assembled system was tested by one prosthesis user in a controlled environment, where the time and force required to move a small object was recorded with and without the haptic feedback engaged.

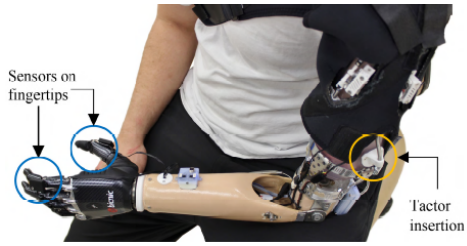

Figure 4.1: Figure of the complete system, integrated into an existing prosthesis. From [25]

4.2.2 Antfolk, C *et. al.*

In [2], a silicone bulb connected via a plastic tube to a silicone pad placed on the skin of the residual limb of several prosthesis users as well as several unimpaired subjects. Contact forces on the fingers of the prosthesis was thus transmitted to the user via air pressure, without the need for electronics or any active components. By placing the actuating bulbs on the phantom maps (2.6), the system achieved somatotopic matching, as well as modality matching, for the subject who had at least a partial phantom map.

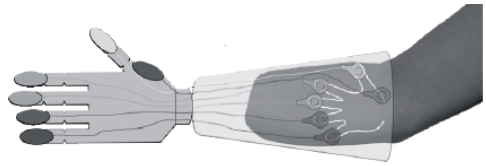

Figure 4.2: Conceptual scetch of the air mediated system from fingertips to phantom map. From [2]

4.2.3 Aboseria, M. *et. al.*

In [1], visual, discrete vibrotactile and continuous normal force feedback, is compared to determine which is most efficiently enables users to regain a stable grip when and object starts to slip. The study's duration was three days, and while it was thought that the continuous feedback of grip force would be more useful, even after three days of training the discrete vibrotactile stimulation was more efficient at preventing object slippage and crushing when regripping.

4.2.4 Barone, D. *el. al.*

In [4], a cosmetic digit, i.e finger, is designed and constructed which includes a FSR, a vibrotactile stimulator, controller and other supporting circuitry. The system is based on the Discrete Event-driven Sensory feedback Control (DESC), discussed in [12]. The vibrational motor was controlled such that it gave a short burst of stimulation whenever an object was grasped or let go. During lab trials, the digit outperformed simple cosmetic prosthesis in a virtual egg test. One digit prosthesis user was given the system to test in their daily life, and anecdotal reports stated that the system was very useful in object manipulation tasks.

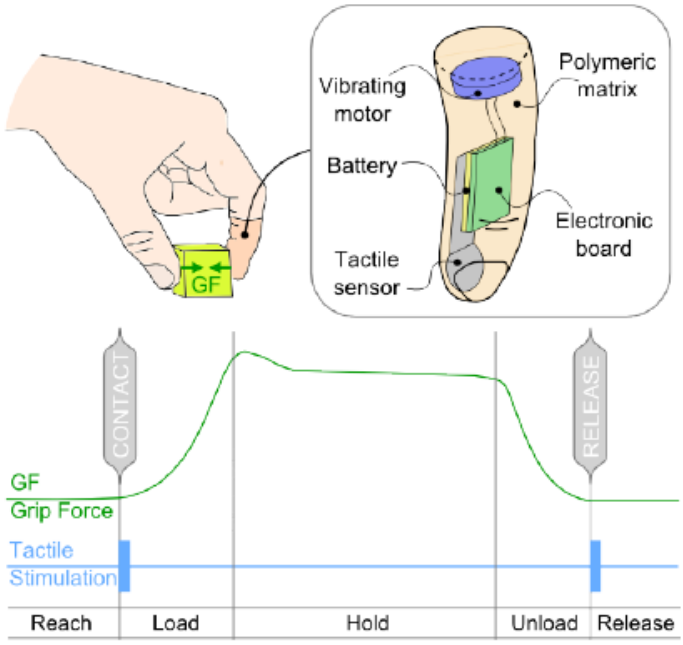

Figure 4.3: Conceptual sketch of the cosmetic digit. Underneath is a time line of the grip force (GF) and the corresponding tactile stimuli. From [4]

CHAPTER

FIVE

PROPOSED ARCHITECTURES

5.1 Sensors on Hand

A system like the one designed and tested in [25], could be implemented for the Hy5 hand, with sensors placed on the fingertips, and under a cosmetic glove. A micro-controller unit (MCU) could be housed within the socket part of the prosthesis. From the MCU actuators placed within the socket can be controlled and tuned. In addition to the control of sensors and actuators, a system with a MCU can include a wireless control interface for tuning even after the system has been installed in the prosthetic system.

The feedback provided by the actuators can be either continuous, or event driven. The events can include object slip, contract with an object, or completing the gripping part of Hy5's adaptive grip , see 3.2.

Pressure sensors could also be embedded within the hydraulic system and the readings from these could be used a the reference signal for the force feedback. Current Hy5 designs only have one high pressure zone, and thus only the average or total pressure of the digits is available for feedback, but should future designs include a separate and controllable zone for the opposing thumb, it should be possible to provide the user with information about the forces in the opposing sides of the hand without the need for exposed sensors.

5.2 Hydraulic or Pneumatic System

As in [2], a simple pneumatic coupling, can be used to give the user information about contact forces. Taking this concept further, utilising the hydraulics in the Hy5 hand to create a pressure on the skin of the prosthesis user could be possible. This would require no additional circuitry, and by only connecting the stimulating pad to the high pressure zone of the hydraulic system in a non looping way the added components would not induce any significant additional flow of hydraulic fluid. While both these variations are simple in their idea, they lack easy tuning and user adaptability other than choosing the stimulation zone.

5.3 Using EMG-signal

An alternative to using force sensors or a fluid to transmit pressures to the user is to give the user tactile information based on the strength of the EMG-signal. While this will not give the user information about the real state of the prosthesis, it will allow the user to gauge his or her signal strength and thereby adjust. While such a system til still require a MCU and actuators, the sensors are already in place as part of the existing prosthetic system.

CHAPTER

SIX

DISCUSSION AND RESULTS

6.1 Discussion of Previous Work

6.1.1 Schoepp, K. *et. al*, see 4.2.1

The system developed by Schoepp and others is of a lightweight and modular design, allowing for easy integration into an already existing prosthetic system. The sensor demonstrates the ability to function and detect changes in applied pressure, even when covered by a nitrile fingertip. While the average force applied to the object when grasping and lifting was reduced when haptic feedback was enabled, the time to complete the task increased. Schoepp argues, in line with other experiments [30], that this difference in time would be reduced given more training time with the haptic feedback, though this is a point of future research.

6.1.2 Antfolk, C *et. al*, see 4.2.2

The idea for the system developed by Antfolk *et. al* dates back to the 1930 [26]. The addition of the feedback system to an existing prosthesis adds little weight and by its passive nature puts no extra load on the battery of the system. Simple in design, and cheap to manufacture, the air pressure system could provide a one size, fits most solution to the haptic feedback problem. However, in it simplicity, the system lacks any real tuning abilities other than pad placement. Also, as demonstrated in [1], discrete vibrational pulses prevented object slip better than continuous feedback.

6.1.3 Barone, D. *et. al*, see 4.2.3

While the feedback system designed was not for a whole hand, but only a finger, it demonstrated how events, communicated through vibration, was an effective tool in motor control. The use of an FSR demonstrated that despite its lacking accuracy, it was useful in determining at least two different events, contact and release, during the lifting and holding of an object.

6.2 Discussion of Proposed Architectures

6.2.1 Sensors on Hand. See 5.1

A system with sensors placed on the fingers of the prosthetic hand will most closely resemble the natural sensor placement of the proposed architectures. [25] demonstrated that a sensor could function under a layer of protective ”skin”, which is vital for the reliability and longevity of a feedback system. For the Hy5 prosthesis, it is proposed that three sensors, on the thumb, index and middle fingers is proposed. These are the fingers which are currently able to move with some degree of independence.

Using a MCU with a communication interface to the outside will allow for personalising of the stimuli to be delivered while the system is in use by the user. The users of such a system will have a varying degree of sensory ability in the residual limb, and thus the sensitivity to different stimuli will vary.

Adding a MCU, several sensors and actuators will clearly increase the weight of the prosthesis. Weight reduction is one of the most cited needs of the users of upper limb prostheses [8]. However, so is sensory feedback, and with the right choice of components the haptic feedback system can hopefully be made lightweight enough such that what is gained can justify the added weight.

The system will draw some power in order to operate the sensors, MCU and actuators. Sourcing the power from battery already included in the system will possibly reduce the time between recharges of the prosthesis. However, as demonstrated in [25], the average grip force was lower when feedback was enabled, thus lowering the power draw of the motor and possibly resulting in a net reduction of power usage.

Adding sensors on two or more of the fingers and covering them with a cosmetic glove could be done, with little to no rework of the actual hand. The MCU, its power supply and the actuators could be housed within the socket part of the prosthesis. Placing actuators on the residual limb would require rework of the area surrounding the skin, and extra work would have to be done when fitting the prosthesis to the user, especially in the presence of a phantom limb map.

Having a pressure sensor within the hydraulics rather than on the fingertips will most likely mean losing the ability to discern much about the shape of objects, as the pressure will only build up to significant levels when the hand has closed around an object. A benefit of such a system is that the sensor no longer is exposed to whatever the hand is touching, and that there will not be a need for cables to run along the moving fingers.

For users where it is possible, actuating areas which correspond to the phantom limb map it thought to be beneficial.

6.2.2 Hydraulic or Pneumatic system. See 5.2

A pneumatic system like the one in [2] is simple, easy to manufacture and can be made cheaply. However, it requires a tube filled with air or some other pressure carrying medium to extend from the fingers to the site of stimulation. This would likely require a significant rework of the current Hy5 design and construction.

The simple system will however lack much of the ability of tuning a system based on a MCU holds. Also, the sensor less system cannot easily be monitored without the addition

of a MCU and sensor array.

6.2.3 Using EMG-signal. See 5.3

This approach is fundamentally different than the two previously proposed, as the source of the feedback is not a force in or on the prosthesis, but rather EMG signal which is used to control what forces are to be generated. While this might not be as useful when using the prosthesis in day to day life, having direct feedback of the EMG signal during training could potentially help users adjust to using the prosthesis.

6.3 Choosing MCU-based system

After having review the literature and proposed and discussed a few architectures, it seems a system controlled by a MCU with sensors in the fingers and actuators on the skin is the best suited for the Hy5 hand. Such a system could inform the user of events during grasping, either directly though changing in normal force stimulation, or through a expanded version of [4], via vibrotactile stimulation. Having a combination of both normal force stimulation for force feedback as well as a vibrotactile stimulator for feedback of motor control events could enable the user to both grip with only the required force as well as prevent object slippage.

A major point of uncertainty is whether users will find the feedback useful or a hindrance when using the prosthesis. Having an added cognitive load might be enough to prompt users to abandon the haptic feedback system. Many studies of haptic feedback are also confined to a laboratory setting, and thus the effect of the added cognitive load might only be apparent in real life trials. If the cognitive load of both normal force stimulation and vibration is proven too great, reverting to only vibrotactile to communicate events is thought to be the better option. Direct nerve stimulation might be a solution to this problem, as, at least in theory, it should be possible to create the same sensations as for individuals not lacking a limb. Failing this, TMSR could be a step closer to somatotopic matching and reduced cognitive load.

The system proposed also only includes force feedback. It is unclear whether proprioception is the missing component in making haptic feedback viable.

CHAPTER
SEVEN

CONCLUSION AND FUTURE WORK

7.1 Conclusion

The system proposed is a MCU-based system with sensors placed in the three of the fingers of the Hy5 prosthesis. There are several uncertain aspects of the proposed system, including: cognitive load, ability to use force sensors to detect events and usability outside of a laboratory setting. The two most important aspects of haptic feedback in motor control seems to be the maintenance of internal forward models and the detection of transitions between states in motor control.

Prosthetic hands is a multidisciplinary field, and the success of any system requires that all parts of the system, from the hand to the fitting of the socket or the surgeon possibly performing osseointegration or TMSR, work together in a compatible way.

7.2 Future Work

Future work will include creating a prototype of the haptic feedback system. This includes hardware as well as software development. An analysis of which events is detectable and communicable to the user with the proposed sensory array and actuators must also be undertaken.

When a prototype has been created, testing the system on prosthesis users in a as realistic scenario as possible is key to determining if the system can be used and commercialised.

BIBLIOGRAPHY

[1] M. Aboseria, F. Clemente, L. Engels, and C. Cipriani. Discrete vibro-tactile feedback prevents object slippage in hand prostheses more intuitively than other modalities. *IEEE Transactions on Neural Systems and Rehabilitation Engieering*, 26:1577–1584, 2018.

[2] C. Antfolk, A. Björkman, S. Frank, F. Sebelius, G. Lundborg, and B. Rosen. Sensory feedback from a prosthetic hand based on airmediated pressure from the hand to the forearm skin. *Journal of Rehabilitation Medicine*, 44:702–707, 2012.

[3] C. Antfolk, M. D'Alonzo, B. Rosén, G. Lundborg, F. Sebelius, and C. Cipriani. Sensory feedback in upper limb prosthetics. *Expert Review of Medical Devices*, 10:45–54, 2013.

[4] D. Barone, M. D'Alonzo, F. Clemente, and Cipriani C. A cosmetic prosthetic digit with bioinspired embedded touch feedback. *ICORR*, pages 1136–1141, 2017.

[5] A. Björkman, A. Weibull, J. Olsrud, H. Ehrsson, Rosén B., and I Björkman-Burtscher. Phantom digit somatotopy: a functional magnetic resonance imaging study in forearm amputees. *European Journal of Neuroscience*, 2012.

[6] M. Catalán. *Towards Natural Control of Artificial Limbs*. PhD thesis, Chalmers University of Technology, 2014.

[7] P. Chapell. Making sense of artificial hands. *Journal of Medical Engieering and Technology*, 35:1–18, 2011.

[8] F. Cordella, A. Ciancio, R. Sacchetti, A. Davalli, A. Cutti, E. Guglielmelli, and L. Zollo. Literature review on needs of upper limb prosthesis users. *Frontiers in Neuroscience*, 2016.

[9] C. Dietrich, K. Walsh, S. Preibler, G. Hofmann, O. Witte, W. Miltner, and T. Weiss. Sensory feedback prosthesis reduces phanom limb pain, proof of a principle. *Neuroscience Letters*, 2012.

[10] S. Dudley and S. Childress. Historical aspects of powered limb prostheses. *Clinical Prosthetics and Orthotics*, 1985.

[11] H. Ehrsson, B. Rosén, A. Stockselius, C. Ragno, P. Köhler, and G. Lundborg. Upper limb amputees can be induced to experience a rubber hand as their own. *Brain*, 2008.

[12] R. Johannson and B. Edin. Predictive feed-forward sensory control during grasping and manipulation in man. *Biomedical Research*, 14:95–106, 1993.

[13] R. Johansson and J. Flanagan. Coding and use of tactile signals from the fingertips in object manipulation tasks. *Nature Reviews*, 10:345–359, 2009.

[14] M. Kawato. Internal models for motor control and trajectory planning. *Current Opinion in Neurobiology*, 1999.

[15] K. Kim, J. Colgate, J. Santos-Munné, A. Makhlin, and M. Peshkin. On the design of miniature haptic devices for upper extremity prosthetics. *IEEE/ASME TRANSACTIONS ON MECHATRONICS*, 15, 2010.

[16] K. Li, Y. Fang, Y. Zhou, and H. Liu. Non-invasive stimulation-based tactile sensation for upper-extremity prosthesis: A review. *IEEE Sensors Journal*, 17:2625–2635, 2017.

[17] C. Lucarotti, C. Oddo, N. Vitiello, and M. Carrozza. Synthetic and bio-artificial tactile sensing: A review. *Sensors*, 13:1435–1466, 2013.

[18] P. Marasco, K. Kim, J. Colgate, M. Peshkin, and T. Kuiken. Robotic touch shifts perception of embodiment to a prosthesis in targeted reinnervation amputees. *Brain*, 2011.

[19] G. Meijer. *Smart Sensor Systems*. Wiley-Interscience, 2008.

[20] A Muzumdar. *Powered Upper Limb Prosthesis*. Springer, 2004.

[21] J. Poirters. Hydraulic pump assembly for artificial hand, 2015. US patent: US20180133032A1.

[22] p. Puangmali, K. Althoefer, L. Seneviratne, D. Murphy, and P. Dasgupta. State-of-the-art in force and tactile sensing for minimally invasive surgery. *IEEE Sensors Journal*, 2008.

[23] E. Romero and D. Elias. Design of a non invasive haptic feedback device for transradial myoelectric upper limb prosthesis. *IEEE ANDESCON*, 2016.

[24] A Rosenbaum. *Human Motor Control*. Academic Press, 1990.

[25] K. Schoepp, M. Dawson, J. Schofield, J. Carey, and J. Herbert. Design and integration of an inexpensive wearable mechanotactile feedback system for myoelectric prostheses. *IEEE Journal of Transtaional Engieering in Health and Medicine*, 6, 2018.

[26] R. Scott. Feedback in myoelectric prostheses. *Clin Orthop Relat Res*, 1990.

[27] A. Serino, M. Akselrod, R. Salomon, R. Maruzzi, M. Belfari, E. Canzoneri, G. Rognini, W. van der Zwaag, M. Iakova, F. Luthi, A. Amoresano, T. Kuiken, and O. Blanke. Upper limb cortical maps in amputees with targeted muscle and sensory reinnervation. *Brain*, 2017.

[28] C. Stray, J. Poirters, and O. Lerstøl-Olsen. Improved prosthetic functionality through advanced hydraulic design. Poster used to display the Hy5 hand and Hy5's philosophy.

[29] D. Tan, M. Schiefer, M. Keith, J. Anderson, J. Tyler, and D. Tyler. A neural interface provides long-term stable natural touch perception. *Science Translational Medicine*, 6, 2014.

[30] H. Witteveen, E. Droog, J. Rietman, and P. Veltink. Vibro- and electrotactile user feedback on hand opening for myoelectric forearm prostheses. *IEEE Transactions on Biomedical Engineering*, 2012.

[31] M. Yiwana, S. Redmond, and N. Lovell. A review of tactile sensing technologies with applications in biomedical engineering. *Sensors and Actuators*, 2012.

Jon Eirik Lisle Andresen

Haptic Feedback for Hydraulic Hand Prosthesis

NTNU
Kunnskap for en bedre verden